DRI No. 2115

AFCRL-63-156

DETERMINATION OF THERMODYNAMIC PROPERTIES OF SEMICONDUCTOR MATERIALS

C. E. Lundin
M. J. Pool
R. W. Sullivan

Denver Research Institute
University of Denver
Denver 10, Colorado

Contract No. AF19(604)-7222
Project 4608

Final Report

28 May 1963

Prepared for
Air Force Cambridge Research Laboratories
Office of Aerospace Research
United States Air Force
Bedford, Massachusetts

AFCRL-63-156

DETERMINATION OF THERMODYNAMIC PROPERTIES OF SEMICONDUCTOR MATERIALS

Contract No. AF19(604)-7222
Project 4608

Prepared for

Air Force Cambridge Research Laboratories
Office of Aerospace Research
United States Air Force
Bedford, Massachusetts

Prepared by

Denver Research Institute
University of Denver
Denver 10, Colorado

Final Report

28 May 1963

APPROVED BY:

William M. Mueller, Head
Metallurgy Division

PREPARED BY:

M. J. Pool
Research Metallurgist

R. W. Sullivan
Research Chemist

C. E. Lundin
Project Supervisor

Requests for additional copies by Agencies of the Department of Defense, their contractors, and other Government agencies should be directed to the:

DEFENSE DOCUMENTATION CENTER (DDC)
ARLINGTON HALL STATION
ARLINGTON 12, VIRGINIA

Department of Defense contractors must be established for DDC services or have their "need-to-know" certified by the cognizant military agency of their project or contract.

All other persons and organizations should apply to the:

U. S. DEPARTMENT OF COMMERCE
OFFICE OF TECHNICAL SERVICES
WASHINGTON 25, D. C.

ABSTRACT

A diphenyl ether calorimeter and a liquid-tin solution calorimeter were employed to determine selected thermodynamic properties of Group III and V elements and their compounds. The enthalpy and heat capacity of eight Group III-V compounds were determined in the solid state. The compounds are: InP, InAs, InSb, GaP, GaAs, GaSb, AlP, and AlSb. Data were obtained on the enthalpy and heat capacity of the liquids of several of these compounds. The heat of fusion was then calculated for these several compounds. The heats of solution of the elements: Al, Ga, In, P, As, and Sb and the compounds: GaSb, InP, InAs, and InSb in tin were determined. From these data the heats of formation of the same compounds were determined.

Knudsen effusion studies were conducted on pure antimony and a series of alloys of the antimony-germanium systems. The vapor pressure of pure antimony was first determined in the range of temperature, 700 to 900C. Vapor pressures and activities of antimony over the mixtures of these alloys were then established. Heats of vaporization for both pure antimony and of antimony over the alloys are presented. The liquid/liquid plus solid boundary of the phase diagram was established from the plot of activity versus mole fraction.

TABLE OF CONTENTS

		Page
I.	INTRODUCTION	1
II.	THERMODYNAMIC PROPERTIES OF INTERMETALLIC COMPOUNDS	3
	A. Heat of Formation	3
	1. Equipment	3
	2. Materials	4
	3. Results and Discussion	4
	B. Heat Contents, Heat Capacities, and Heat of Fusion	7
	1. Equipment	7
	2. Materials	8
	3. Results and Discussion	8
III.	KNUDSEN EFFUSION STUDIES	13
	A. Equipment	13
	1. Knudsen Apparatus	13
	2. Effusion Cells	14
	B. Materials	15
	C. Results and Discussion	16
	1. Knudsen Effusion Technique	16
	2. Design Studies	17
	3. Vapor Pressure of Antimony	24
	4. The Thermodynamics of the Germanium-Antimony System	24
	REFERENCES	29
	ACKNOWLEDGEMENTS	30
	APPENDIX	

I. INTRODUCTION

This final report with the research work described herein is submitted in compliance with the terms of Contract No. AF19(604)-7222 between the Air Force Cambridge Research Laboratories, Electronic Systems Division, United States Air Force and the Denver Research Institute, University of Denver (Colorado Seminary). The report period is inclusive of 1 April 1960 to 30 April 1963. The program is entitled "Determination of Thermodynamic Properties of Semiconductor Materials."

The objective of this research effort was to provide thermodynamic property data for selected materials of semiconductor application. The program was three phase in scope. The first phase of the study was directed toward the design and construction of suitable apparatus to obtain the thermodynamic data. The apparatus to be built consisted of a liquid-tin solution calorimeter and a Knudsen effusion apparatus. The third piece of equipment that was employed, a diphenyl ether calorimeter, was available from the initiation of this program. The second phase of the effort was to determine the enthalpy and heat capacity of the Group III-V intermediate phases in the solid phase and also in the liquid phase, where possible. The heat of fusion of these phases was determined when the melting point of the intermediate phase was within the temperature range of the equipment. These data were determined using the diphenyl ether calorimeter. Inclusive in the second phase was the determination of the heats of solution of the Group III and the Group V elements in tin. The heats of solution of the Group III-V intermediate phases in tin were then determined. Using these data, the heats of formation of the Group III-V intermediate phases were calculated. The heat of solution values were obtained with the liquid-tin solution calorimeter. The third phase of the program involved a Knudsen effusion technique study of the vapor pressures of antimony vapor over antimony-germanium alloys in the liquid and liquid plus solid solution region of the diagram in the temperature range of 700 to 900C. From this information, a plot of activity versus mole fraction was determined and the boundary of the liquid/liquid plus solid region was established. The heat of vaporization data calculated from the slopes of the $\log_{10} p$ versus $1/T$ plot indicated that the vapor species of antimony over the alloy are the same as the vapor species of the pure antimony. Also, included in the third phase of the study was a rather comprehensive evaluation of various crucible designs and materials, heating techniques, and techniques of obtaining vapor pressure data by the Knudsen effusion technique.

A survey of the literature was conducted during the first part of the program and published as Scientific Report No. 1 through the Air Force Cambridge Research Laboratories. The survey was entitled "Literature Survey of Selected Semiconductor Properties," AFCRL 4, 1 December 1960. This information was used as a basis for evaluating and establishing the types of thermodynamic data which were lacking and the priority of determining the properties of the various materials on this program.

II. THERMODYNAMIC PROPERTIES OF INTERMETALLIC COMPOUNDS

A. Heat of Formation

1. Equipment

An isothermal, liquid-metal solution calorimeter was constructed to measure the heats of formation of intermetallic compounds. The calorimeter, which is shown in Figure 1, was designed to operate at temperatures up to approximately 500° C; any metals with melting points below this temperature can be used as solvents. Ideally, a solvent should have a low melting point, a low vapor pressure, and a well-established heat capacity. It should also be available in a pure form. Tin has been employed in this calorimeter since it meets the above requirements and is sufficiently economical to permit extensive use.

The calorimeter has given excellent temperature control. The maximum drift in temperature of the calorimeter is about 0.2° C per day, and an attempt to measure the temperature cycling in the calorimeter itself indicated no measurable fluctuations; i.e., less than 0.002° C.

When a sample is dropped into the liquid-metal bath, an endothermic or an exothermic reaction occurs. This causes a temperature change in the bath, and a temporary temperature difference is established between the bath and the aluminum calorimeter block. The magnitude and duration of the temperature perturbation is directly related to the heat of solution.

In order to get a large EMF for a given temperature change, a multijunction thermopile is used for each of the calorimeter wells. Forty-eight of the thermopile junctions are distributed over the surface of the calorimeter and serve to integrate the heat effects occurring. The other forty-eight are next to an aluminum calorimeter block. In the operation of the calorimeter, two thermopiles are always used; one is termed the active well and the other passive. The thermopiles are connected differentially so that any change in temperature of the outer junctions (which will be the same for both wells because of the high conductivity of the aluminum block) will oppose the two wells and result in no shift of the zero. The electrical output is thus the true temperature difference between the two reaction vessels. A reaction occurring in the active well gives a comparison with another body of very similar thermal properties. In this way, any spurious heat effect due to slight temperature drifts within the entire calorimeter block is eliminated.

In the initial design of the calorimeter an Ar-H_2 gas mixture was used to prevent excessive oxidation of the bath. However, the heat transfer characteristics proved to be disadvantageous. The calorimeter was changed so that any pair of wells could be evacuated simultaneously. The modified top is shown in Figure 2. Also apparent in this figure is the constant temperature ice bath in which the sample is held before being dropped into the calorimeter.

2. Materials

All of the materials used in this work were of the highest purity available. The pure metals had a minimum purity of 99.99%. The compounds were semiconductor grade and had a minimum purity of 99.99%. No deviation from stoichiometry was found in the compounds.

3. Results and Discussion

The heats of solution of the six elements: aluminum, gallium, indium, phosphorous, arsenic and antimony have been determined by liquid metal solution calorimetry. The solvent used for all elements was liquid tin. The temperature of dissolution in all cases was 750 ± 1°K. The results are presented in Table I as the average value of the partial molar heat of solution. The error given was calculated from the standard deviation of all values from the average value.

Table I

Partial Molar Heats of Solution of Elements

Element	No. of Runs	ΔH Meas. (cal/g-atom)	$\overline{\Delta H}_{750}$ (cal/g-atom)	Error
Al	20	9160	6075	± 40
Ga	11	5265	765	± 25
In	13	3870	-250	± 20
P	7	9035	5820	±100
As	8	6030	2990	± 30
Sb	20	6775	3720	± 35

Previous work has been done by Cohen et al.[1] on the heats of solution of aluminum, gallium and indium in tin at 575 and 625°K. Kleppa[2,3] has also determined the heats of solution of gallium and indium in liquid tin. The results of these two investigations agree within experimental error with the results of this investigation except in the case of

indium. Both Cohen and Kleppa report a value for indium less exothermic than the value obtained in this work. The discrepancy can easily be accounted for since the heat of solution for indium is the difference between two numbers both of which are approximately 4000. A small error in the measured value could give an extremely large error in the calculated difference which is the heat of solution. It should also be noted that the mean error for indium is of the order of ten percent even though the absolute value is smaller than any of the others.

No analysis of the experimental data could be made from the standpoint of the theories of dilute solutions. In order to carry out an analysis of this type, a concentration dependent partial molar heat of solution must be obtained. In no case was any concentration dependency found. Cohen et al. did find a concentration dependent partial molar heat of solution for aluminum but the dependency was slight.

There appears to be a definite trend in the heat of solution of both the Group III and Group V elements. If Cohen's data for thallium are used, it is seen that the heats of solution of the Group III elements go through a minimum at indium. Even though no data are available for bismuth, it appears that the Group V elements will go through a minimum at arsenic. Since these values are associated with the tin-group III or V phase diagrams, it appears that no compounds will be found in the tin-arsenic or tin-phosphorous phase diagrams. This conclusion is based on the fact that tin does not form compounds with aluminum, gallium or thallium, all of which have positive heats of solution but does form one or more compounds with indium, which has a negative heat of solution.

The heats of solution of four of the nine III-V compounds were also determined. The compounds which would dissolve in liquid tin at 750°K were InAs, InP, InSb, and GaSb. The rate of solution for the compounds GaAs, GaP, AlP, and AlSb were so slow that no reliable data could be obtained. The compound AlAs could not be obtained commercially. The partial molar heat of solution at 750°K could be determined since the heat contents of these compounds were determined simultaneously with the determination of the heats of solution. The measured values of the heat of solution when the sample was added from 273°K along with the values at 750°K obtained by subtracting the difference in heat contents between 273°K and 750°K are tabulated in Table II.

Table II

Partial Molal Heats of Solution of Compounds

Compound	No. of Runs	ΔH Meas. (cal/g-atom)	$\overline{\Delta H}_{750}$ (cal/g-atom)	Error
GaSb	15	10,900	7,792	± 60
InP	6	13,700	10,800	± 100
InAs	17	12,098	9,298	± 100
InSb	13	8,984	5,968	± 50

The data obtained for the heats of solutions have been used to calculate the heats of formation of the compounds at two different temperatures. The method of calculation is based on the following reactions for the solution of the constituent elements and the compound.

$$A(T = 273°K) \rightarrow \underline{A}\,(T = 750°K)\ \Delta H_1$$

$$B(T = 273°K) \rightarrow \underline{B}\,(T = 750°K)\ \Delta H_2$$

$$AB(T = 273°K) \rightarrow \underline{A} + \underline{B}\,(T = 750°K)\ \Delta H_3$$

The ΔH's used for these reactions are the measured ΔH's, and the heat of formation is referred to 273°K. If the heat contents at 750°K of the constituent elements and the compound are subtracted from the measured ΔH's then the reactions of concern are:

$$A(T = 750°K) \rightarrow \underline{A}\,(T = 750°K)\ \Delta H'_1$$

$$B(T = 750°K) \rightarrow \underline{B}\,(T = 750°K)\ \Delta H'_2$$

$$AB(T = 750°K) \rightarrow \underline{A} + \underline{B}\,(T = 750°K)\ \Delta H'_3$$

In this case the partial molar heats of solutions at 750°K are used for the $\Delta H'$s. Regardless of which method is used the heat of formation referred to the initial temperature of the elements and compounds is given by:

$$\Delta H_{fT} = \frac{\Delta H_1 + \Delta H_2}{2} - \Delta H_3$$

The factor of 2 in the first term is introduced in order to base the calculated heat of formation on 1 gram-atom (6×10^{23} atoms) of compound. The values for the heat of formation at both 273°K and 750°K are given in Table III.

Table III

Heats of Formation of III-V Compounds

Compound	$\Delta H_{f(273)}$ (cal/g-atom)	$\Delta H_{f(750)}$ (cal/g-atom)
InP	-7250 ± 220	-8015 ± 220
InAs	-7148 ± 150	-7928 ± 150
InSb	-3661 ± 100	-4233 ± 100
GaSb	-4880 ± 110	-5554 ± 110

The values for InSb, GaSb and InAs can be compared to the values obtained by Schottky and Bever.[4] All of the values are to be compared at 273°K. For InSb the corresponding value is -3470 ±110 cal/g-atom; for InAs, -7400 ± 640 cal/g-atom; and for GaSb, -4970 ± 220 cal/g-atom. In all three cases the agreement between the two sets of data is well within experimental error. The value for indium phosphide is the only known one available.

Again it is apparent that a trend exists within each group. For instance when the Group III element indium is combined with phosphorous, arsenic and antimony, it is seen that the heat of formation decreases upon going down through Group V. This apparently is also related to the melting points of the compounds which decrease in the same fashion. The same trend is also apparent if the Group V element is the same and the group III element is variable.

B. Heat Contents, Heat Capacities, and Heat of Fusion

1. Equipment

A diphenyl-ether calorimeter was constructed to measure the high-temperature heat contents and heat capacities of intermetallic compounds. This calorimeter is shown in Figure 3. The calorimeter operates on the same principle as an isothermal Bunsen ice-calorimeter, but is more sensitive due to the large volume change which occurs upon melting of the calorimetric substance.

The calorimeter is surrounded by a thermostatically controlled mineral-oil bath which is maintained slightly above the melting point of diphenyl ether (300.03K). The bell jar containing the calorimeter well and diphenyl ether is surrounded by a larger diameter bell jar which serves to damp out thermal fluctuations in the mineral-oil bath. A

nichrome-wound tube-furnace containing a large stainless steel block which holds the sample prior to dropping is mounted above the calorimeter. The stainless steel drop mechanism is evacuated to prevent oxidation of the sample, and a thermocouple is set into the stainless steel block in close proximity to the specimen. When the sample is dropped, it follows a curved path and then drops through a spring-loaded, stainless-steel radiation gate into the calorimeter well. The curved path and the radiation gate both prevent radiant energy from the furnace reaching the calorimeter well. The calorimeter well is separated from outside of the calorimeter by a thin-walled stainless steel tube in order to reduce heat transfer in this direction. The calorimeter well consists of a heavy 1 1/4 in. -diam copper tube with 1/16 in. -thick copper discs soldered to it at 1/2 in. intervals. This facilitates both the freezing of the solid mantle and the distribution of heat during a run. The well contains a copper-screen basket surrounded by copper lathe turnings. This facilitates rapid heat transfer from the specimen to the calorimeter well. (Argon is also added after the drop to speed heat transfer.)

Since both solid and liquid ether are maintained at the melting point throughout the run, essentially all the heat contained in the specimen is used to melt a portion of the solid mantle. The expansion which accompanies this melting forces part of the mercury contained in a pool in the bottom of the calorimeter out through a stainless steel tube connected to a 28-ft. length of calibrated capillary tubing.

2. Materials

The materials used for this phase of the work were the same as those used for solution calorimetry.

3. Results and Discussion

The heat contents of the eight group III-V compounds AlP, AlSb, GaP, GaAs, GaSb, InP, InAs and InSb have been determined from 300°K to 1300°K. The equipment and experimental method have been discussed under the equipment section. The results are presented graphically in Figures 4 through 11. The curves have been treated with a least squares analysis to yield equations of the form,

$$H_T - H_{300} = A + BT + CT^2.$$

The coefficients of the equation for each compound are listed in Table IV. The relative heat content has units of calories/g-atom.

Table IV

Heat Content Equations for III-V Compounds

Compound	A	B	C
AlP	-1706	5.58	3.43×10^{-4}
AlSb	-1830	5.99	3.75×10^{-4}
GaP	-1692	5.58	2.06×10^{-4}
GaAs	-1719	5.65	2.61×10^{-4}
$GaSb_{(s)}$	-1855	6.15	1.11×10^{-4}
$GaSb_{(\ell)}$	7940	4.32	---
InP	-1832	6.05	2.03×10^{-4}
InAs	-1737	5.69	3.36×10^{-4}
$InSb_{(s)}$	-1960	6.60	-2.08×10^{-4}
$InSb_{(\ell)}$	3630	6.65	---

Smoothed values of the heat contents at 100° intervals are given in Table V. These values were calculated from the best fit equations of Table IV.

In order to establish a criterion for the validity of the data the heat contents of three standards were also measured over approximately the same temperature range. The curves for these standards are plotted in Figures 12 to 14. For all three standards the measured heat content was below the accepted value, the degree of deviation being a function of temperature. An average correction factor was determined from the standard data, and this factor was applied to the data for all compounds. The low values apparently are a result of radiative heat losses during the time the specimen is falling from the furnace into the calorimeter. Since conditions are essentially the same for all drops from any one temperature, the use of an average correction factor is sound.

The heat capacities for all eight compounds have also been determined by taking the first derivative of the heat content equations with respect to temperature. In this case the heat capacity is a linear function of temperature. A comparison of the heat capacity of any one compound with the sum of the heat capacities of its constituent elements shows that a negative deviation from the Kopp-Neumann rule occurs for all compounds. This is a good indication that the Debye temperature has been increased by formation of the compound and that the bond strengths are reasonably high. Another indication of this general trend is the relatively high heats of formation discussed previously.

Table V

Relative Heat Contents for the III-V Compounds

Compound	Temp. °K	$H_T - H_{300.15}$ cal/gm. atom
AlP	400	580
	500	1175
	600	1770
	700	2375
	800	2980
	900	3600
	1000	4220
	1100	4840
	1200	----
AlSb	400	610
	500	1248
	600	1890
	700	2545
	800	3200
	900	3860
	1000	4540
	1100	5210
	1150	5550
GaP	400	580
	500	1165
	600	1745
	700	2330
	800	2920
	900	3510
	1000	4110
	1100	4720
	1200	5330
GaAs	400	575
	500	1165
	600	1760
	700	2360
	800	2970
	900	3580
	1000	4195
	1100	4820
	1200	5440
	1250	5750

Table V (cont'd)

Compound	Temp. °K	$H_T - H_{300.15}$ cal/gm. atom
$GaSb_{(s)}$	400	620
	500	1230
	600	1855
	700	2475
	800	3005
	900	3730
$GaSb_{(\ell)}$	1000	12260
	1100	12680
	1200	13340
InP	400	612
	500	1237
	600	1865
	700	2500
	800	3130
	900	3775
	1000	4420
	1100	5065
	1200	5715
InAs	400	575
	500	1180
	600	1790
	700	2405
	800	3030
	900	3655
	1000	4280
	1100	4925
	1200	5575
$InSb_{(s)}$	400	645
	500	1280
	600	1922
	700	2555
	800	3180
$InSb_{(\ell)}$	803	8960
	900	9615
	1000	10275
	1100	10955

The heats of fusion have also been determined for the compounds GaSb, InSb and InAs. The values in kilocalories/g-atom are 7.9, 5.8 and 7.0. These values were obtained by taking the difference between the heat contents of the liquid and the solid at the published melting point. The value for indium arsenide is based on one point obtained in the liquid region. The heat content at the melting point was obtained by assuming that the heat capacity of the liquid was equal to the heat capacity of the solid and drawing a line through the one point with the appropriate slope. Vieland[5] has estimated the heat of fusion of indium arsenide and obtained a value of 7.2 Kcal/g-atom. The value obtained in this work should be reasonably close to the true value.

Schottky and Bever[4] have measured the heats of fusion of InSb and GaSb by quantitative thermal analysis. They obtained values of 6.1 Kcal/g-atom for InSb and 6.0 Kcal/g-atom for GaSb. Nachtrieb[6] has also determined the heat of fusion for InSb by drop calorimetry. His value is 5.61 Kcal/g-atom. The value obtained in this work is between these two values and falls within the limits of error of both.

The heat of fusion of GaSb found in this investigation is considerably higher than that found by Schottky and Bever. No reasonable explanation for this difference is available. However, if the same trend occurs in the heat of fusion as in the heat of formation it would be expected that the heat of fusion for GaSb would be greater than that of InSb.

III. KNUDSEN EFFUSION STUDIES

A. Equipment

1. Knudsen Apparatus

The Knudsen effusion apparatus which was used for vapor pressure studies on this program was designed and constructed at Denver Research Institute. The apparatus and associated controls are shown pictorially in Figure 15. The control panel can be seen at the left of the apparatus in the photograph. A Minneapolis-Honeywell Brown Electronik temperature recorder-controller is mounted at the top of the panel. The furnace unit employs resistance heating, and the recorder-controller maintains the temperature within ± 1°C of the control temperature at 900°C during the on-off control cycle. All of the electrical controls for the recorder-controller, the furnace unit, and both vacuum pumps are located on the control panel in addition to water valves which control the cooling water to the furnace unit and the diffusion pump. A voltmeter measures the potential on the primaries of the power transformers, and an ammeter measures the current in the main tungsten heater circuit.

The furnace unit consists of a water-cooled brass shell with a sight port and shutter assembly to allow temperature measurement with an optical pyrometer. Both ends of the furnace shell have flanges to accommodate 'O'-ring vacuum seals. The top of the furnace shell is attached to the bottom of an aluminum plate which serves as the base plate for the Pyrex bell jar. The furnace base plate and furnace components are shown in Figure 16. The components in ascending order in the photograph are: a stainless-steel tripod, molybdenum plate, alumina pedestal, graphite effusion cell, tungsten heating coil, alumina cover, and tantalum heat shields. The furnace base plate as shown in the photograph contains two glass-insulated electrical leads. During the course of the program it was necessary to add a second spiral tungsten heater and two additional glass-insulated electrical leads. As a result the present base plate has four electrical leads instead of the two shown in the photograph. An eight conductor Amphenol plug is mounted in the center of the base plate; this allows as many as four thermocouples to be used inside the furnace chamber. The base plate is also water-cooled. The Pyrex bell jar provides vacuum continuity between the furnace chamber and the high-vacuum source.

The tungsten spiral heaters were fabricated from stranded tungsten wire (3 strands each 0.025 in. diameter). Power for the heater coils is supplied by American Transformer Company filament transformers. Power to the auxiliary heater coil is supplied by a single transformer; the voltage on the primary of this transformer is regulated by a Variac. The main heater coil power is supplied by two filament transformers wired in parallel. Control is achieved by operating one transformer in series with the recorder-controller. This arrangement allows continuous heating to a temperature slightly below the desired operating temperature, and the additional heating current is supplied during the "on" cycle of the recorder-controller. The output of these transformers is 190 amperes at 5.2 volts.

The high-vacuum source for the apparatus is provided by a Welsh Duo-Seal mechanical pump, a Consolidated Electrodynamics Corporation PMC-720 oil diffusion pump, and a liquid nitrogen cold trap. The system can be operated with or without liquid nitrogen in the cold trap. A vacuum of 5×10^{-6} Torr is attainable without liquid nitrogen, and a vacuum of 2×10^{-7} Torr is attained when using liquid nitrogen. The apparatus is equipped with both a thermocouple and an ion gauge to measure the system vacuum.

A target wheel assembly is mounted on the bell-jar base plate. The target wheel will accommodate eight targets, each 2-1/8 in. diameter. This assembly is shown pictorially in Figure 17. This multiple target holder permits seven individual vapor pressure determinations to be made with a single loading of the apparatus. The wheel can be rotated magnetically from outside the bell jar. For reasons described in the section of this report on Design Studies, the target technique of determining vapor pressure was not used. All of the data reported were obtained by means of the crucible weight-loss technique.

2. Effusion Cells

The design of the effusion cell used on this program is shown in Figure 18. The individual cells used to study the germanium-antimony system were fabricated entirely from tantalum metal. The outside shells of the cells were made from 1/2 in. O.D. tantalum tubing with a 0.015 in. wall thickness. The thermocouple wells were made from 3/16 in. O.D. tubing with a 0.010 in. wall thickness. The tops of the thermocouple wells were crimped closed and then welded as indicated in the drawing. The cell bottoms and lids were machined

from 1/2 in. diameter tantalum rod. All joints were Heliarc welded and then helium leak tested to insure against leaks in the cells. The only opening in a finished cell was the orifice itself. The temperature of the cell was obtained by spot welding a chromel/alumel thermocouple to the thermocouple well wall by discharging a condenser bank through the thermocouple as the tip was brought in contact with the well.

The effusion cell used to determine the vapor pressure of pure antimony was fabricated from pyrolytic graphite. The basic design was the same as that of the tantalum cells. However, the lid could not be welded to the body of the cell, and a pressed fit was employed in the design to obtain a vapor-tight seal.

B. Materials

Three materials were employed in this phase of the study; these were silver, germanium, and antimony. The silver was used as a means of calibrating the Knudsen effusion apparatus, both from the standpoint of temperature and vapor pressure. Since the melting point and vapor pressure of silver are rather well established, silver provided an excellent pure material with which to conduct the necessary initial equipment calibrations. The silver was obtained from The Consolidated Mining and Smelting Company of Canada, Limited, and is in the form of pellets. The silver is "Tadanac" brand with a purity of 99.9999 percent silver. The germanium was obtained from Sylvania Electric Products, Inc. It is polycrystalline, transistor-grade germanium and is specified by the manufacturer to have a minimum resistivity of 40 ohm/cm. at 27°C. The germanium was obtained in one of the manufacturer's standard ingot forms. The antimony was obtained from The Bunker Hill Company. It is transistor grade, high-purity antimony. The typical analysis is as follows.

Pb - 10 ppm

Cu - 10 ppm

Fe - 10 ppm

As - 10 ppm

Sb - 99.9996 w/o by difference

The antimony was in ingot form.

C. Results and Discussion

1. Knudsen Effusion Technique

The Knudsen effusion technique is frequently employed to determine vapor pressures in the pressure range below 1 mm Torr. This technique involves the determination of the amount of vapor effusing through an orifice of known area in a measured time period. The effusing species must be known, and the assumption is made that the vapor behaves as an ideal gas at the low pressures involved. The effusion orifice is assumed to be a point source for the effusing vapor. From a kinetic consideration of the behavior of an ideal gas the following equation which expresses the vapor pressure in terms of experimental parameters can be derived,

$$P = \frac{t}{a} k \sqrt{\frac{2\pi RT}{M}}, \quad \text{where}$$

P is the vapor pressure in the millimeters of mercury,

t is the rate of vapor effusion in grams per second,

a is the orifice area in square centimeters,

k is a unit conversion constant,

R is the ideal gas constant in dynes per square centimeter,

T is the temperature in degrees Kelvin, and

M is the molecular weight of the effusing species.

In practice the amount of vapor effused in a given time is usually determined by one of two methods. In the first method the effusion cell containing the material whose vapor pressure is to be determined is weighed before and after a vapor pressure determination. The weight loss of the effusion cell represents the weight of vapor effused during the determination. This method was used on this program to obtain the vapor pressure data on both the pure antimony and the germanium-antimony alloys.

In the second method a cold target is suspended directly above the effusion orifice and in a plane parallel to the plane of the orifice. Both the orifice to target distance and the target radius must be accurately known. If the effusing species has an accommodation coefficient of one when striking the target material, all of the vapor

molecules striking the target will condense and remain on the target. Under these conditions the fraction of the effusing vapor found on the target can be calculated from the cosine distribution law according to the following formula,

$$f = \frac{r^2}{r^2 + d^2} \quad ,$$

where f is the vapor fraction, r is the target radius, and d is the orifice to target distance. The expression for the vapor pressure of the effusing species now becomes,

$$P = \frac{t}{af} k \sqrt{\frac{2\pi RT}{M}} \quad .$$

If the effusing vapor actually conforms to a cosine distribution, the vapor pressure as determined by either method will be the same. It also follows that if the vapor pressure is determined by both methods on the same experimental run, the weight loss of the effusion cell multiplied by the vapor fraction will equal the amount of material collected on the target.

2. Design Studies

When the Knudsen apparatus was designed at the beginning of this program, the target wheel assembly was incorporated to allow multiple vapor pressure determinations to be made with a single loading of the apparatus. As designed, one position on the sample wheel was to be used as a shutter position. The remaining seven target positions could be used for seven vapor pressure determinations employing the target technique. This arrangement would eliminate the evacuation time and the heat-up and cool-down time required for each individual vapor pressure determination when using the cell weight-loss technique. This design was also compatible with the use of radioisotopes in that the targets could be removed from the Knudsen apparatus and counted directly with no further processing.

When the apparatus was first placed in operation high-purity silver in a tantalum effusion cell was used to calibrate the apparatus. Reliable data were available in the literature on both the vapor pressure and the melting point of silver, and this provided a convenient means of checking both the effusion apparatus design and the accuracy of the temperature measurements. During the calibration of the apparatus

the vapor pressure of silver was determined by both the target and the cell weight-loss techniques on each individual vapor pressure determination.

The melting point of silver determined in the effusion apparatus was lower than the accepted value by 4 to 6C. The indicated melting point was observed on each vapor pressure determination, and the appropriate temperature correction was made at the operating temperature of each vapor pressure determination.

The vapor pressure of silver determined by the cell weight-loss technique agreed very well with the accepted vapor pressure reported in the literature.[7,8,9,10] Figure 19 is a plot of the experimental points, and the curve is a least squares fit of the experimental points. Analysis of the data results in the following mathematical expression for silver vapor pressure in the temperature interval from 980 to 1225C:

$$\log_{10} P(\text{mm Hg}) = -\frac{14,249 \pm 237}{T} + 8.93 \pm 0.17.$$

The heat of vaporization as calculated from the slope is: $\Delta H = 62,200$ cal/mole.

The vapor pressure of silver as determined by the target technique was consistently higher than the pressure determined by the cell weight-loss technique. On the initial determinations the target technique yielded results high by a factor of almost two. Critical examination of the experimental techniques failed to reveal any logical explanation of these results. A cosine distribution of the effused vapor had been assumed; the results indicated this was a false assumption.

The actual distribution of the effused vapor in the Knudsen apparatus was determined by the following technique. A "target stack" consisting of thirteen individual concentric targets ranging in diameter from 3.499 inches to 0.158 inches was fabricated. The targets were made from stainless steel sheet 0.020 inches thick. Each target had a small hole in the center, and the stack could be held together by means of a small bolt and nut. The bolt head was flat and fit flush with the face of the adjacent target; thus, the bolt head itself was the smallest target. From the weight of silver collected on the exposed area of each target, a weight-to-area ratio could be determined. From the inside and outside diameters of the exposed target area, the angle included by a line passing through the center of the exposed target area and the orifice with the normal to the orifice could be determined. These data could then be plotted to obtain the actual distribution pattern

of the effused vapor. Figure 20 is a plot of that distribution pattern. Superimposed is a plot of the normal cosine distribution. The normal distribution is positioned on the plot to indicate the approximate weight-to-area ratios that could be expected if the effusing vapor had in fact conformed to a normal cosine distribution. From a comparison of the two plots it can be readily seen that considerable focusing of the effusing beam was being produced by the heat shield configuration.

A number of design changes were investigated in an effort to eliminate the focusing of the effusing vapor beam. The top and side heat shield arrangement that produced focusing of the beam can be seen in Figure 16. With the heat shields in place, a large portion of the effusing beam was intercepted by the top heat shield stack. The compartment formed by the heat shields in effect acted as a second effusion cell; the portion of the beam intercepted by the top heat shields was free to condense and reevaporate from the inner heat shield surfaces until a portion of it eventually reached the target. The focusing effect was considerably reduced by large openings in the bottom portion of the side heat shields and by enlarging the opening in the top heat shield so that less of the effusing beam was intercepted by it. A combination of these two changes produced vapor pressure values by the target technique which were only 15 percent higher than the values obtained by the cell weight-loss technique.

An ideal cell design would have no obstructions between the plane of the effusion orifice and the target. A number of vapor pressure determinations were made with no top heat shield in place. The heat loss using this arrangement was so great that there was a sufficient thermal gradient between the melt and the effusion cell lid that at the conclusion of an experimental run the entire melt was condensed on the cell lid. In order to eliminate this thermal gradient and at the same time leave a free path between orifice and target, an improved heating technique was required.

A new furnace base plate and shell were fabricated. The furnace shell incorporated a sight port and shutter arrangement to allow temperature measurements by optical pyrometry. The base plate had two hollow glass-insulated electrical leads in addition to the two solid electrical leads. A three-turn induction coil was fabricated from flattened 3/16 inch O.D. copper refrigeration tubing. An Ajax 6 KW induction heating unit was used as a power source. The induction coil was positioned concentric with and outside the tungsten spiral heater,

and the center turn of the induction coil was level with the effusion cell lid. The temperature was controlled in the normal manner by the recorder-controller.

The effused vapor pattern produced when using this apparatus geometry is shown in Figure 21. For this experiment a graphite effusion cell containing pure antimony was used. A small tantalum disc with an opening in the center was placed on top of the effusion cell lid. The tantalum was a better susceptor than the graphite, and more efficient heating of the cell lid could be obtained by use of the disc. In Figure 21 the effused vapor pattern indicated that some focusing was still being produced. However, this apparatus geometry resulted in target vapor pressure values approximately 15 percent higher than cell weight-loss values. When using the original apparatus geometry, this discrepancy was from 80 to 90 percent.

The combination of induction and resistance heating was not particularly successful from the standpoint of stability. The system was subject to very erratic temperature fluctuations, and at times these fluctuations were so great that temperature control was lost. The induction unit was usually operated at a low power output, and the small coil size required to fit inside the furnace shell represented a very inefficient load for this particular unit. The instability of this combined system was such that precise temperature control appeared impractical if not impossible, and an alternate method of heating the cell lid was designed.

The hollow electrical leads in the furnace base plate were replaced with solid leads identical with those used for the main heater. A second tungsten spiral heater consisting of only two turns and larger in diameter than the main heater was fabricated. It was positioned concentric with and slightly above the main heater. The resistance of this auxiliary heater was less than that of the main heater, and as as result it could be operated at a higher temperature for the same voltage input. It was necessary to use a single top heat shield to eliminate the temperature gradient between the melt and the effusion cell lid, and also, to prevent excessive heating of the targets and target wheel. By proper manipulation of the power input to both heaters the melt and the effusion cell lid could be maintained at the same temperature, and no further difficulty was experienced with material condensing at the orifice. This apparatus geometry resulted in target vapor pressure values still approximately 15 percent higher than the vapor pressure as determined by the cell weight-loss technique on the same determination.

For this reason, and others to be described later, the data reported herein were obtained by the cell weight-loss technique. The double tungsten heater arrangement was adopted as the most suitable method of heating and controlling the temperature of the effusion cell.

The vapor pressure of silver was determined using a welded tantalum effusion cell. At the conclusion of the apparatus calibration with the silver, the determination of the vapor pressures of pure germanium and pure antimony was begun using tantalum as the effusion cell material. Both germanium and antimony severely attacked the tantalum. In a period of minutes in the temperature range 900 to 950C the germanium had diffused through the 0.010 inch wall of the thermocouple well and caused failure of the thermocouple. The rate of attack of the antimony was slower, but it was evident that tantalum was not a suitable material to contain either molten antimony above 900C or molten germanium at any temperature in the liquid state.

Effusion cells were fabricated from high-density, degassed, spectroscopic grade graphite rod which had been obtained from United Carbon Products, Incorporated. Neither the germanium nor the antimony attacked the graphite, and the vapor pressures of both pure germanium and pure antimony were determined using this material for the effusion cells and using the weight-loss technique. The vapor pressure values for both materials were significantly higher than values reported in the literature. In view of the results obtained with silver during the calibration of the apparatus, it was decided to check the graphite for porosity. This was accomplished by evacuating an effusion cell in a vacuum flask and then seating a lid with no orifice in it in place by means of a push rod. The graphite lid could not be welded to the body of the cell, so it was attached by a tapered pressed fit as had been done with the other graphite cells. There was no indication of vapor escaping around the cell lid during the experimental runs. Several determinations with the closed effusion cell revealed that as much antimony was escaping through the walls of the effusion cell during a vapor pressure determination as was escaping through the orifice. Subsequent microscopic examination of the walls of the effusion cell revealed tiny droplets of metallic antimony in the pores of the outside wall of the effusion cell. Because of this porosity this particular type of graphite was considered unsuitable as effusion cell material.

Other materials were then investigated for possible use for effusion cell fabrication. One of the first materials investigated was

"Lavite" purchased from the American Lava Corporation. In the green or unfired condition this material is very soft and can be easily machined. This material is hydrous aluminum silicate, and after firing and dehydration during the firing, it becomes very hard and has considerable strength. It was known before the testing started that this material had some porosity. At temperatures above 800°C the porosity of the "Lavite" approached that of the graphite, and as a result this material was eliminated from further consideration.

Several effusion cells were fabricated from boron nitride. After 4 or 5 experimental runs the boron nitride became severely discolored. Calculations involving the free energy of formation of boron nitride and antimony nitride at the temperatures of the vapor pressure determinations showed that thermodynamically it was possible for antimony vapor to attack boron nitride and reduce it to elemental boron. Because of the possibility of attack and, also, the fact that the antimony vapor pressure values obtained when using boron nitride cells were high, boron nitride was rejected as an effusion cell material.

A number of quartz effusion cells were fabricated and tested. The fabrication of quartz cells was very difficult; much time and effort was spent in developing techniques to fabricate small orifices with a knife-edge in the cell lid which could then be attached to the cell body. Antimony did not attack the quartz, and a series of 5 vapor pressure determinations were made with one quartz cell. At the conclusion of the fifth determination it was observed that the orifice edges had begun to chip, and small particles of the cell lid had fallen into the cell. Several of the quartz cells failed where the bottom had been joined to the side of the cell. Because of the difficulty of fabrication and the unreliability of the finished cell the use of quartz for effusion cell fabrication was abandoned.

Tungsten was the next material investigated. One effusion cell was fabricated from sintered, hot swaged tungsten rod. Improper design of the lid necessitated the use of excessive heat when the lid was welded to the body of the cell, and this resulted in partial oxidation of the antimony charge. However, a number of vapor pressure determinations were made with this cell, and there was no apparent attack of the tungsten by the antimony.

Single crystal tungsten was obtained for the fabrication of additional effusion cells. The supplier claimed that this material could be fabricated by the use of normal machine shop procedures. The

single cyrstal tungsten rod could be easily cut with an alumina cut-off disc, but attempts to surface grind cylinders cut from the rod resulted in a very fine crack across the diameter of the cylinder. Attempts to machine this material at room temperature resulted in severe chipping. Since high temperature machining facilities were not available, no further effort was made to fabricate an effusion cell from the single crystal tungsten.

One attempt was made to fabricate an effusion cell from the sintered, swaged tungsten rod by the electro-erosion machining technique. Very fine cracks were found in the side walls of the finished cell. A number of voids were observed in a cross section of this material. The cost of fabrication by this method was very high. Due to the poor quality of the swaged rod and the excessive fabrication costs, the use of tungsten for effusion cell fabrication was abandoned.

Pyrolytic graphite was obtained from High Temperature Materials, Incorporated, and effusion cells were fabricated from this material. As with the porous graphite, a tapered pressed fit was employed to attach the lid to the body of the effusion cell. A lid with no orifice in it was fabricated, and three experimental runs were made to determine the vapor loss around the pressed fit. Although there was a slight vapor loss on these runs, the loss was negligible in comparison with the amount of vapor lost on a normal vapor pressure determination. The material was not porous and was not attacked by molten antimony. The vapor pressure of pure antimony was determined using a pyrolytic graphite effusion cell.

Preliminary runs with a germanium-antimony alloy indicated a strong negative deviation from ideality with a resultant reduced activity of both components when alloyed. It was believed that welded tantalum effusion cells might be used for the alloy system in the temperature range 700 to 900C. Subsequent experiments showed that tantalum could be used with the alloy system; however, several effusion cells failed after prolonged use at 850 and 900C. The use of the tantalum effusion cells had two advantages: 1) There was no uncertainty as to whether there was a vapor-tight seal between the cell lid and body, and 2) the thermocouple could be welded to the thermocouple well to give a positive thermal contact which could not be done with a pyrolytic graphite cell.

3. Vapor Pressure of Antimony

The vapor pressure of pure antimony was determined in the temperature range 650 to 950C. A pyrolytic graphite effusion cell was used with a 0.0046 in. diam. orifice. Because it was impossible to obtain a knife edge around the circumference of the graphite orifice, the cross section of the cell lid where the orifice was drilled was 0.006 in. thick. A refinement of Clausing's table of correction factors published by S. P. Detkov[11] was used to make a correction for the orifice geometry.

Figure 22 is a plot of the experimentally determined vapor pressure points. Only one determination was made at 650°C. At all other temperatures at least two determinations were made. Analysis of these data lead to the following equation for the vapor pressure of antimony,

$$\log_{10} P = - \frac{6220}{T} + 6.12.$$

The heat of vaporization is +28.5 kcal per mole. This value agrees well with the value +29.3 kcal per mole reported by Illarionov and Cherepanova[12] and a value of +28.4 kcal per mole at 1000°K calculated by Richards.[13]

4. The Thermodynamics of the Germanium-Antimony System

Nine alloys were prepared by 10 w/o increments from 90 w/o germanium to 20 w/o germanium by weighing and melting appropriate charges of the components in evacuated quartz capsules. The capsules were heated in a tube furnace to 50°C above the liquidus temperature to assure complete mixing and melting of the alloys. The temperature range over which the studies of the germanium-antimony system were conducted was from 700 to 900°C at 50°C intervals. The studies were carried out by a series of Knudsen effusion experiments. Each alloy composition was heated in an effusion cell to the desired temperature level and allowed to effuse vapor for an appropriate time interval. From the weight loss of the crucible, the quantity of the effusing vapor was determined. The nine alloys were each allowed to effuse at each of five temperature levels. Therefore, forty-five separate experiments were involved. To check the reproducibility and to provide a good statistical average, each experiment was repeated at least three times, in most cases. A total of 108 effusion runs were conducted throughout the temperature interval of 700 to 900°C and the composition range of 90 to 10 w/o germanium. Since a phase diagram has been determined for this system by other techniques,[14,15] the diagram was used as a general guide in formulating the program. The program was designed to cover the regions of liquid solution and liquid plus germanium solid solution.

The vapor pressure of antimony is sufficient orders of magnitude greater than germanium at the same temperature that the quantity of germanium effused is negligibly small. The total weight loss during each experiment was thus attributed to antimony. The vapor pressure of antimony over the alloy mixture can then be calculated using the relationship as described in a previous section:

$$p(\text{mm of Hg}) = \frac{t}{a} k \sqrt{\frac{2\pi R T}{M}}$$

Each experiment was designed so that the length of the time at the effusing temperature was long enough to reduce the heating and cooling time-errors to a negligible fraction of the total. A temperature calibration was conducted twice during each experiment by recording the thermal analysis curve both on heating and on cooling. The solidus temperature (eutectic temperature) for all germanium-antimony alloys, 590C, could be easily detected and served as a good indication of the temperature consistency of the entire run. The tantalum crucibles were prepared so that one crucible would be used for each alloy throughout the temperature range, 700 to 900C. The orifice size had to be closely matched to the alloy composition. In general, as the alloy composition became richer in antimony, the orifice size was made smaller in order to maintain the best Knudsen conditions in the effusion cell and of the vapor effusing through the orifice. The diameter of the orifice was calculated to size at the temperature of each run by taking into account the thermal expansion of tantalum. The orifice size varied from about 0.008 in. for the 20 w/o germanium alloy to about 0.030 in. for the 90 w/o germanium alloy.

The vapor pressures of antimony over the alloy mixtures at each temperature were calculated, and the average value for each set of at least three runs were plotted as ln p(mm of Hg) versus the reciprocal of absolute temperature. Figure 23 presents these data. Isochores or lines of constant composition are drawn through each alloy composition from 20 to 60 w/o germanium. This region of the phase diagram is the all liquid region. The slope of these isochores represents the heat of vaporization of antimony from the liquid mixture. The values of the heats of vaporization are presented in Table VI below.

Table VI

Heat of Vaporization of Antimony from the Liquid Alloys

Alloy Composition, w/o Ge	ΔH_V, Kcal/mole
20	28.0
30	27.4
40	29.1
50	30.4

The average value of these slopes is 28.7 Kcal/mole which compares favorably with that of pure antimony, 28.4 Kcal/mole in the same temperature region. Thus, one can make a valid assumption that the vapor species is the same effusing from the alloys as it is from pure antimony, namely tetra-atomic. A series of alloys were also investigated by mass spectrometry in a cursory manner to determine if there was a change in the vapor species. This experiment also confirmed that the species did not change for pure antimony and a 20 w/o antimony alloy.

The equations representing the relationships involved in calculating the vapor pressure of antimony over the alloys are presented in Table VII.

Table VII

Equations of Lines of the Isochores in the Germanium-Antimony System

Alloy Composition, w/o Ge	Equation of Isochore
20	$\log_{10} p\,(\text{mm of Hg}) = -\frac{6330}{T} + 5.72$
30	$\log_{10} p = -\frac{6000}{T} + 5.16$
40	$\log_{10} p = -\frac{6360}{T} + 5.24$
50	$\log_{10} p = -\frac{6670}{T} + 5.12$

The intersection of the isochores with the lower line in Figure 23 represents the phase boundary between the liquid and the liquid plus solid regions. Thus, this lower line is the two-phase region where the composition may vary but the vapor pressure and the temperature remain constant. A plot of the liquidus boundary from these data is presented in Figure 24, which also shows the phase diagram as determined

by other techniques. There is reasonably good agreement between the two liquidus boundaries. From the plot in Figure 23, values of vapor pressure were taken at constant temperature at 700, 750, 800, 850, and 900C. The activity of antimony in the alloy solution was then calculated using the vapor pressure of pure antimony at the same temperature and assuming ideal gaseous conditions existing. The activity, in turn, was then plotted versus mole fraction of the alloy composition in Figure 25. The data used to determine the plot of Figure 25 are presented in Table VIII below.

Table VIII

Data Required for Activity Calculation

Temperature, °C	w/o Ge	Vapor Pressure Sb Over Alloy, mm Hg	Vapor Pressure, Pure Antimony, mm Hg	Activity
700	80	0.17	0.52	0.32
	75	0.13	0.52	0.25
750	80	0.34	1.10	0.32
	70	0.21	1.10	0.18
	60	0.20	1.10	0.11
800	80	0.670	2.13	0.32
	70	0.368	2.13	0.17
	60	0.174	2.13	0.08
	54	0.111	2.13	0.05
850	80	1.22	3.88	0.32
	70	0.66	3.88	0.17
	60	0.32	3.88	0.08
	50	0.16	3.88	0.04
	42	0.10	3.88	0.03
900	80	2.11	6.60	0.32
	70	1.13	6.60	0.17
	60	0.56	6.60	0.08
	50	0.26	6.60	0.04
	30	0.10	6.60	0.02

A family of activity plots were established in this manner. As can be seen the activity curve in the single-phase liquid region coincides at all temperatures. In other words, the activity in the liquid phase does not vary with temperature. Whereas, in the two-phase region of liquid plus

germanium solid solution, the activity at each temperature becomes constant for varying composition. Also, in this same region the activity varies with temperature. Since the solid solubility is extremely limited, the activity plots in the two-phase region extend almost to pure germanium. The deviation from Raoult's Law is negative in the liquid solution and positive in the germanium solid solution due to the characteristics of the phase equilibria.

In both Figures 23 and 25, the data in the high-temperature and germanium-rich regions were not plotted because of the larger degree of scatter. This is attributed to some reaction with the tantalum crucibles, because, in some cases, the alloys in this region reacted with the welds. Below 900C and at compositions less than 60 w/o germanium negligible reaction occurred. This was substantiated by metallographic analysis and also fluorescent X-ray analysis of the alloy after a series of runs. Even though the data of the antimony-rich alloys and pure antimony in the temperature region near 900°C were taken under conditions presumably poor for effusion under molecular flow conditions, the data fit rather well on the plots shown in Figures 23 and 25. Therefore, it is felt that if any deviations existed they were not serious.

References

1. J. B. Cohen, B. W. Howlett, and M. B. Bever, Trans. AIME, 221, p. 683 (1961).
2. O. J. Kleppa and R. C. King, Acta Met., 10, p. 1183 (1962).
3. O. J. Kleppa, J. Phys. Chem., 60, p. 842 (1956).
4. W. F. Schottky and M. B. Bever, Acta Met., 6, p. 320 (1958).
5. L. J. Vieland, Acta Met., 11, p. 137 (1963).
6. N. H. Nachtrieb and N. Clement, J. Phys. Chem., 62, p. 876 (1958).
7. C. L. McCabe and C. E. Birchenall, Trans. AIME, 197, p. 707 (1953).
8. P. L. Woolf, G. R. Zellars, E. Foerster, and J. P. Morris, Report of Investigations #5634, Bureau of Mines, 1960.
9. J. Fisher, Z. anorg. u. allgem. Chemie, 219, p. 367 (1934).
10. H. von Wartenberg, Z. anorg. u. allgem. Chemie, 56, p. 320 (1908).
11. S. P. Detkov, Zhur. Fiz. Khim., 34, p. 1634 (1960). In English as AEC-TR-4348.
12. V. V. Illarionov and A. S. Cherepanova, Doklady Akad. Nauk SSSR, 133, p. 1086 (1960).
13. A. W. Richards, "Physical Chemistry of Process Metallurgy, Part I," AIME Metallurgical Society Conference, Vol. 7, Edited by George R. St. Pierre, Interscience Publishers, Inc., New York, 1961.
14. K. Ruttewit and G. Masing, Z. Metallkunde, 32, p. 52 (1940).
15. H. Stöhr and W. Klemm, Z. anorg. Chem., 244, p. 205 (1940).

Acknowledgements

The contribution to the program by Mr. Ronald Cox, Graduate Research Associate, is greatly appreciated. Also, gratitude for the work of the two technicians, Mr. Hugh Warren and Mr. Richard Burrows, must be expressed. In the early stages of the program, contributions to the effort were provided by Mr. Richard Seibel, Research Metallurgist, and Mr. Richard Guadagno, Graduate Research Associate.

APPENDIX

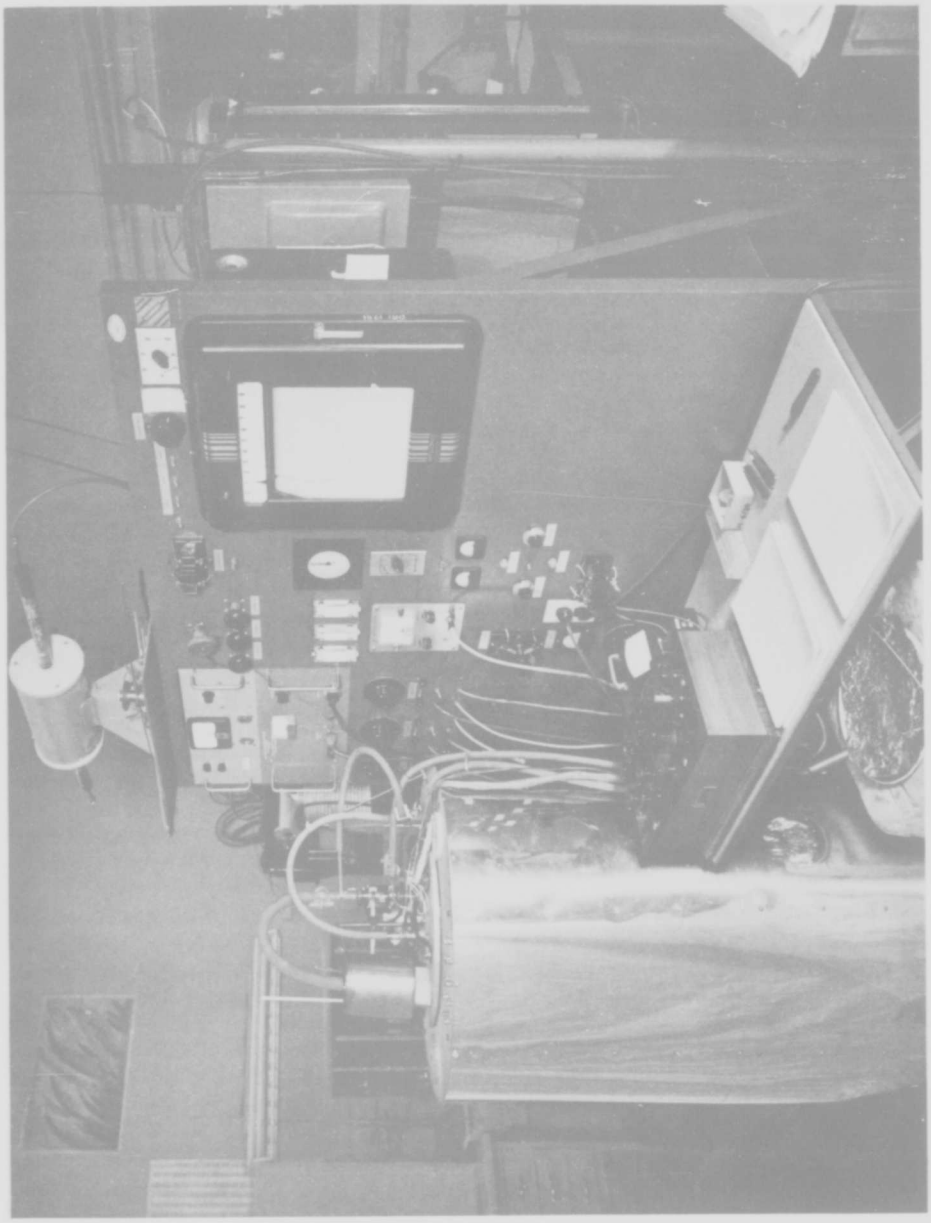

Figure 1. Liquid-Metal Solution Calorimeter.

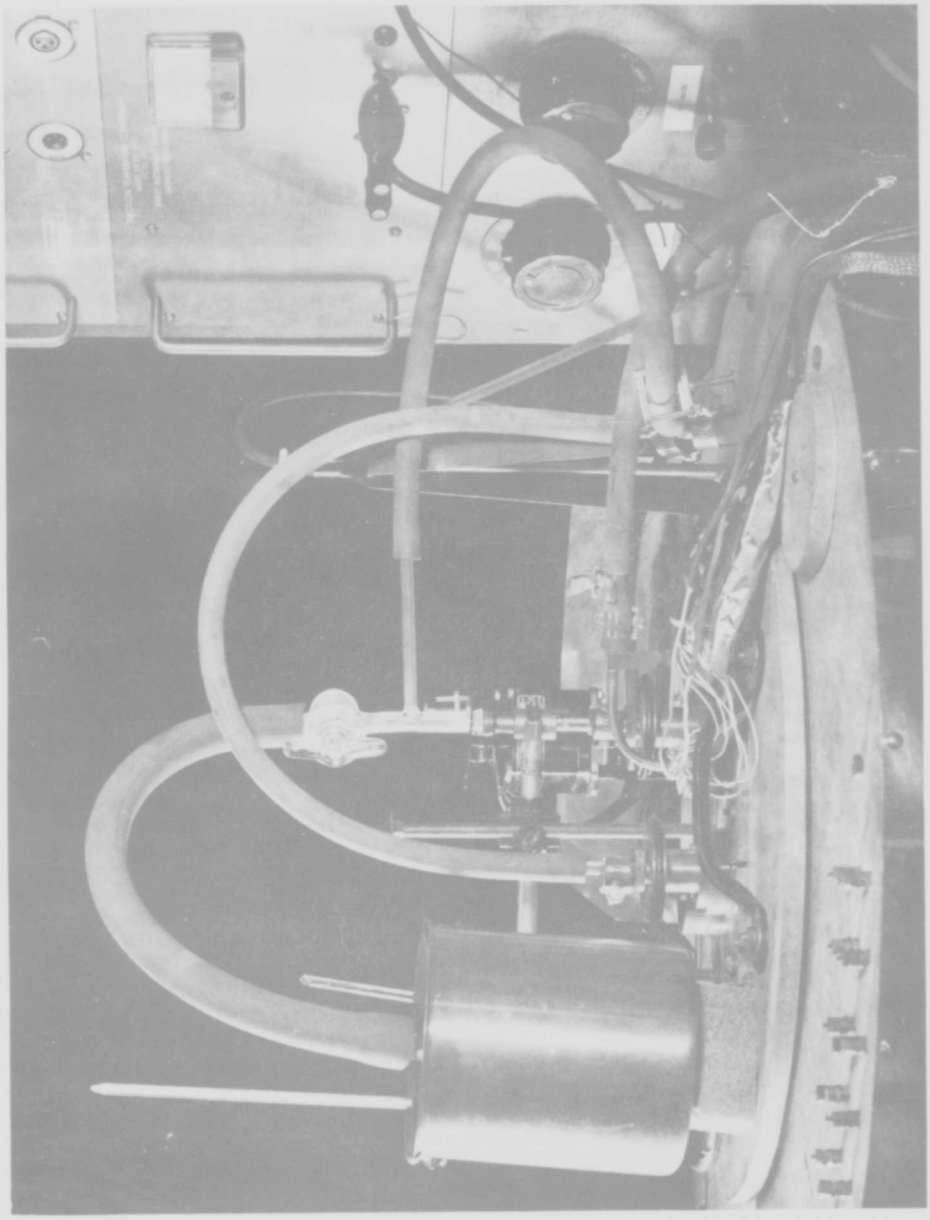

Figure 2. Evacuating System on Liquid-Metal Solution Calorimeter.

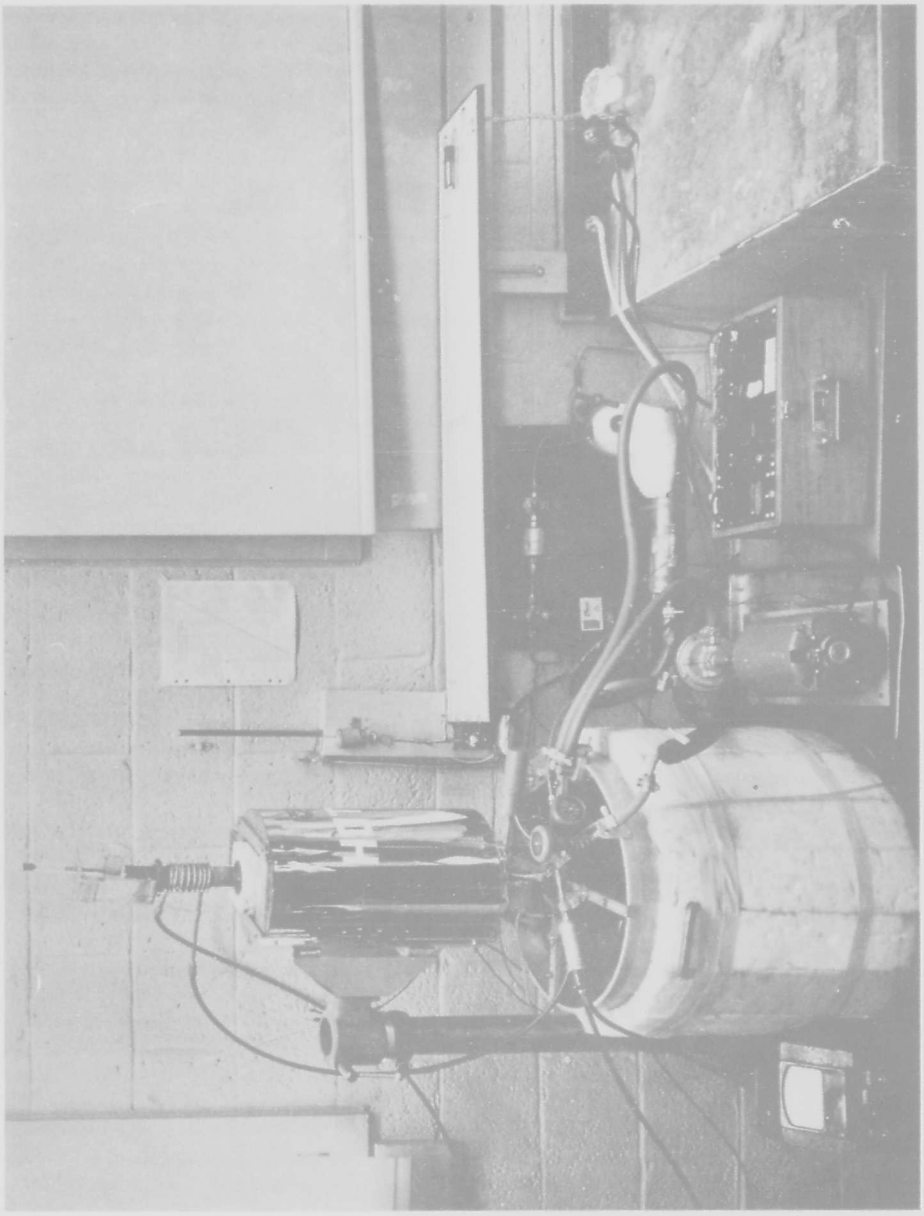

Figure 3. Diphenyl-Ether Calorimeter.

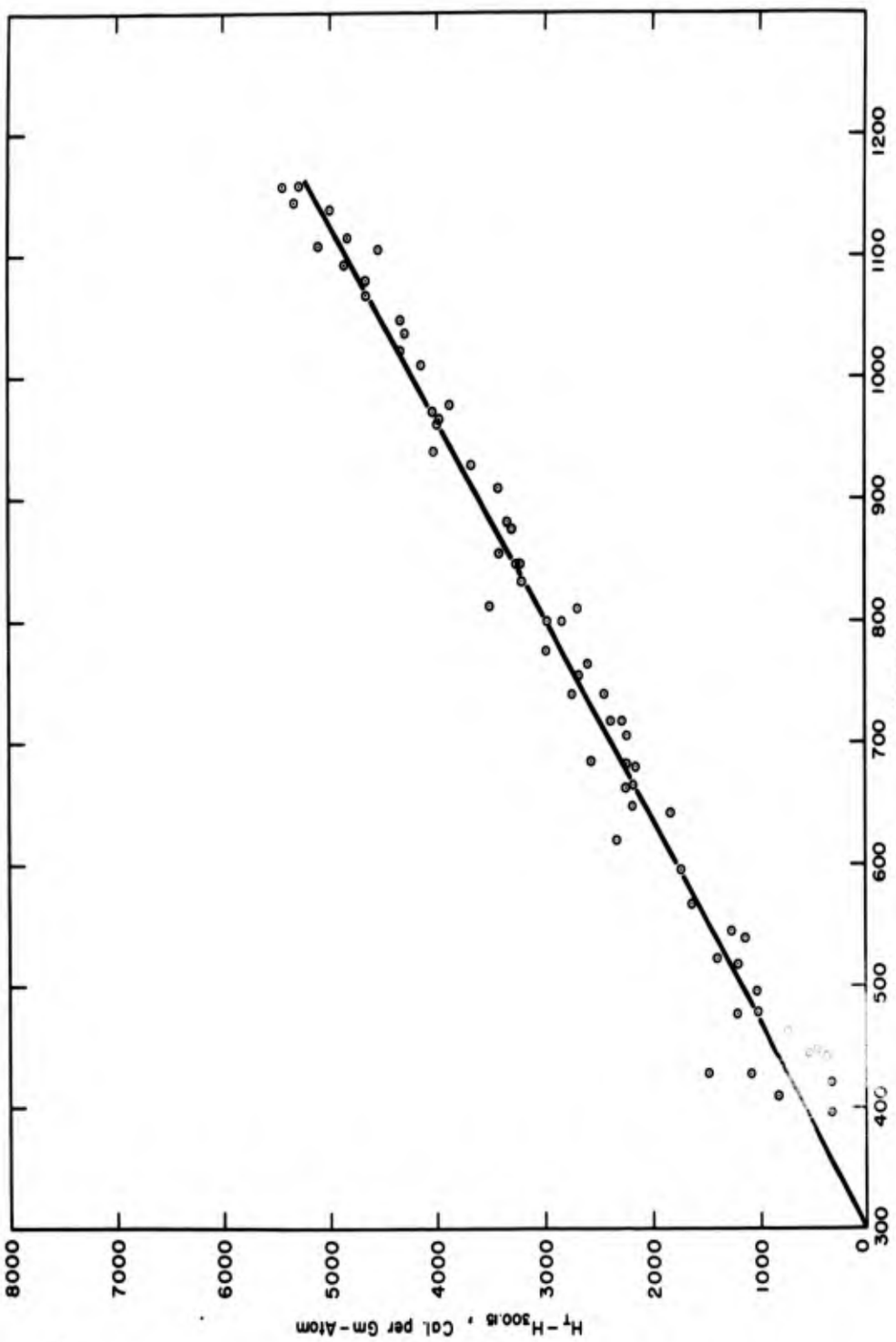

Figure 4. Heat Content of AlP.

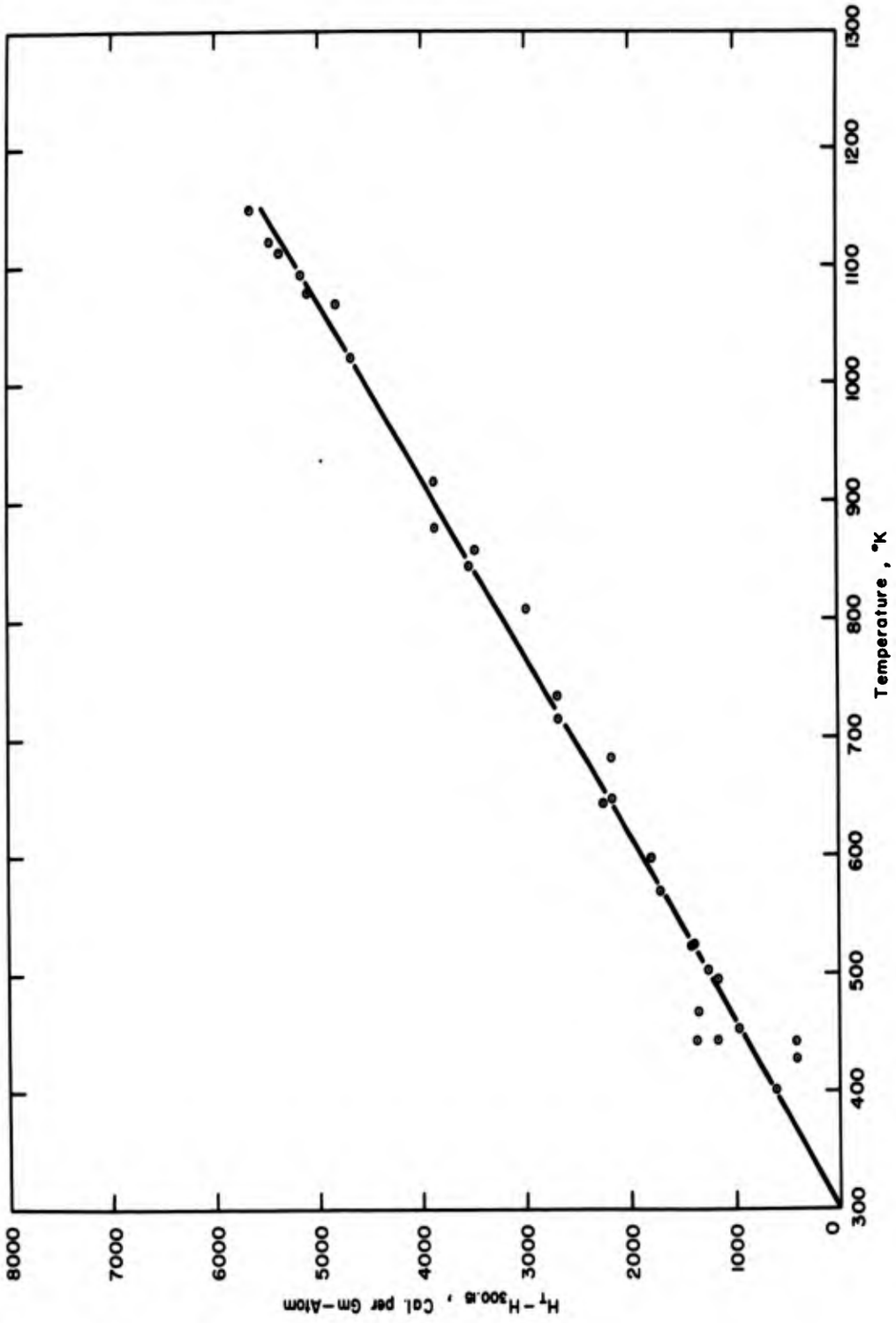

Figure 5. Heat Content of AlSb.

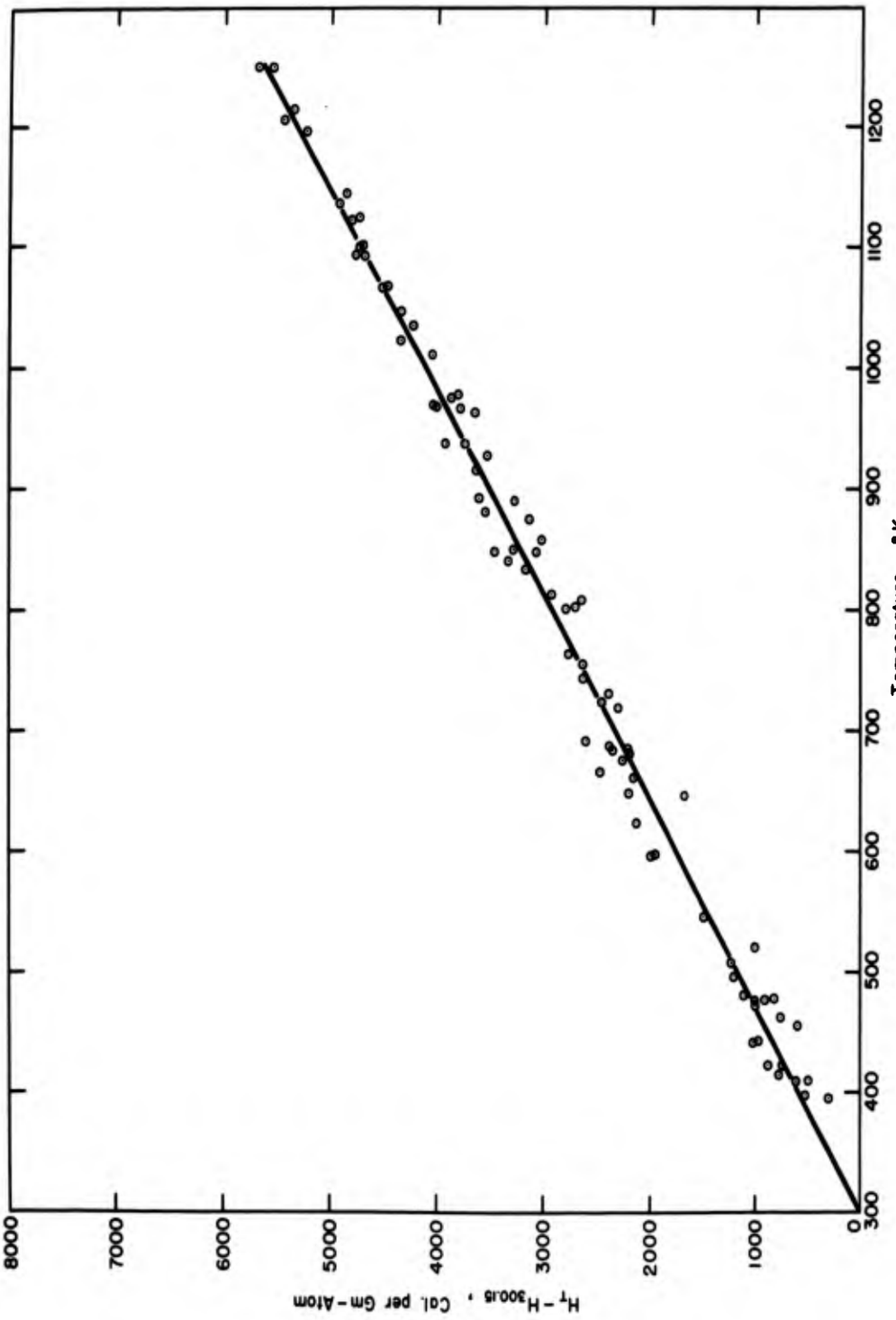

Figure 6. Heat Content of GaP.

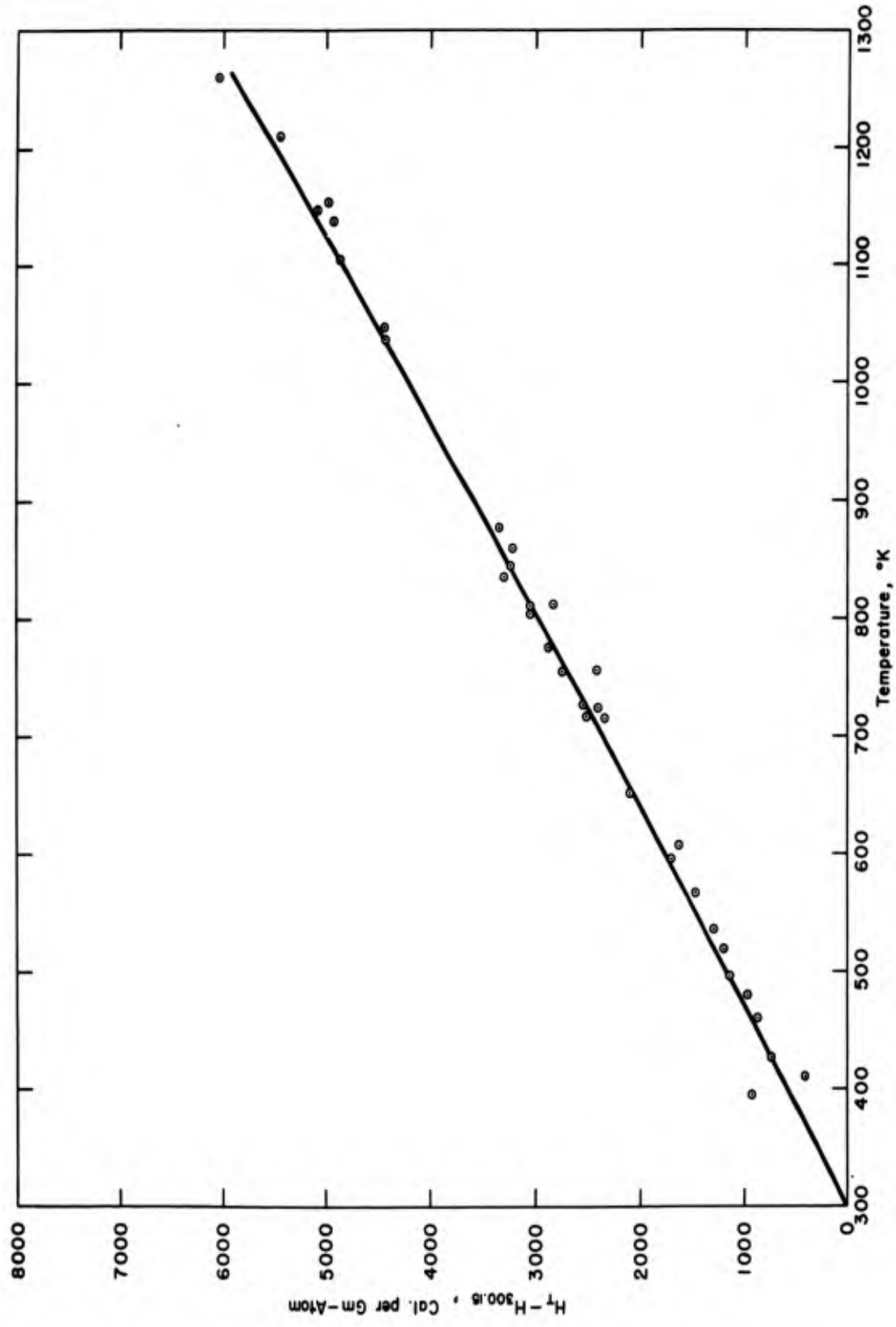

Figure 7. Heat Content of GaAs.

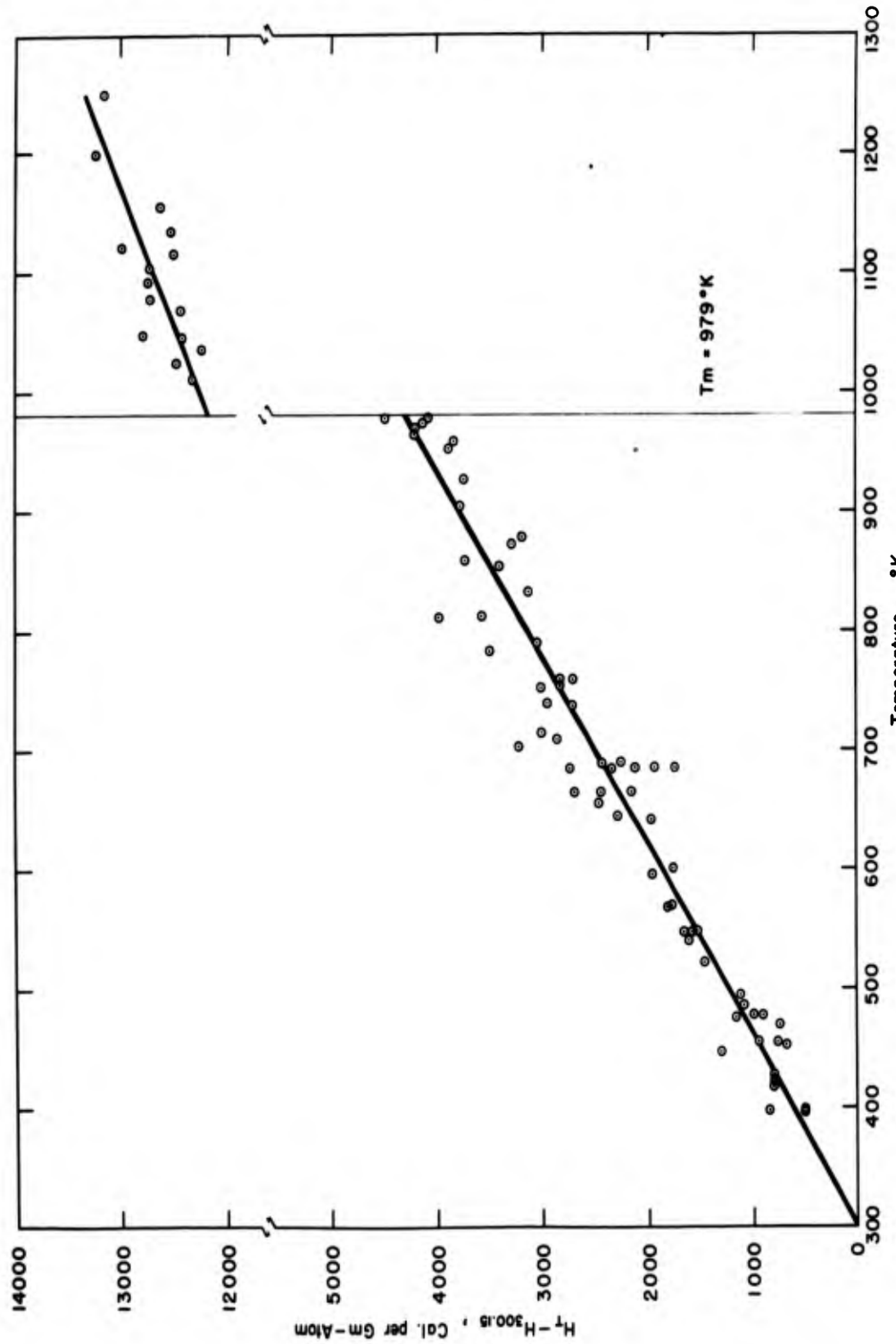

Figure 8. Heat Content of GaSb.

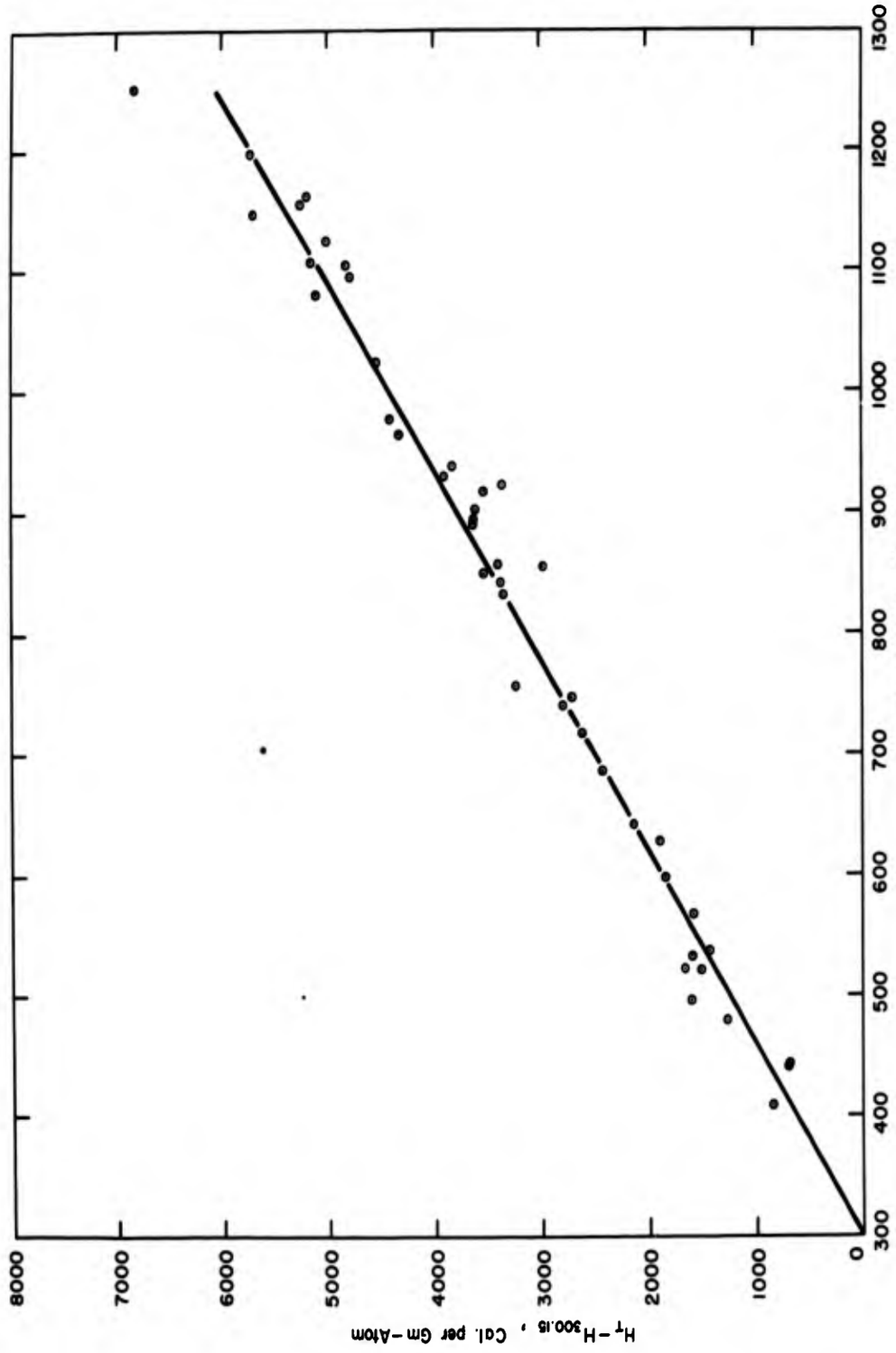

Figure 9. Heat Content of InP.

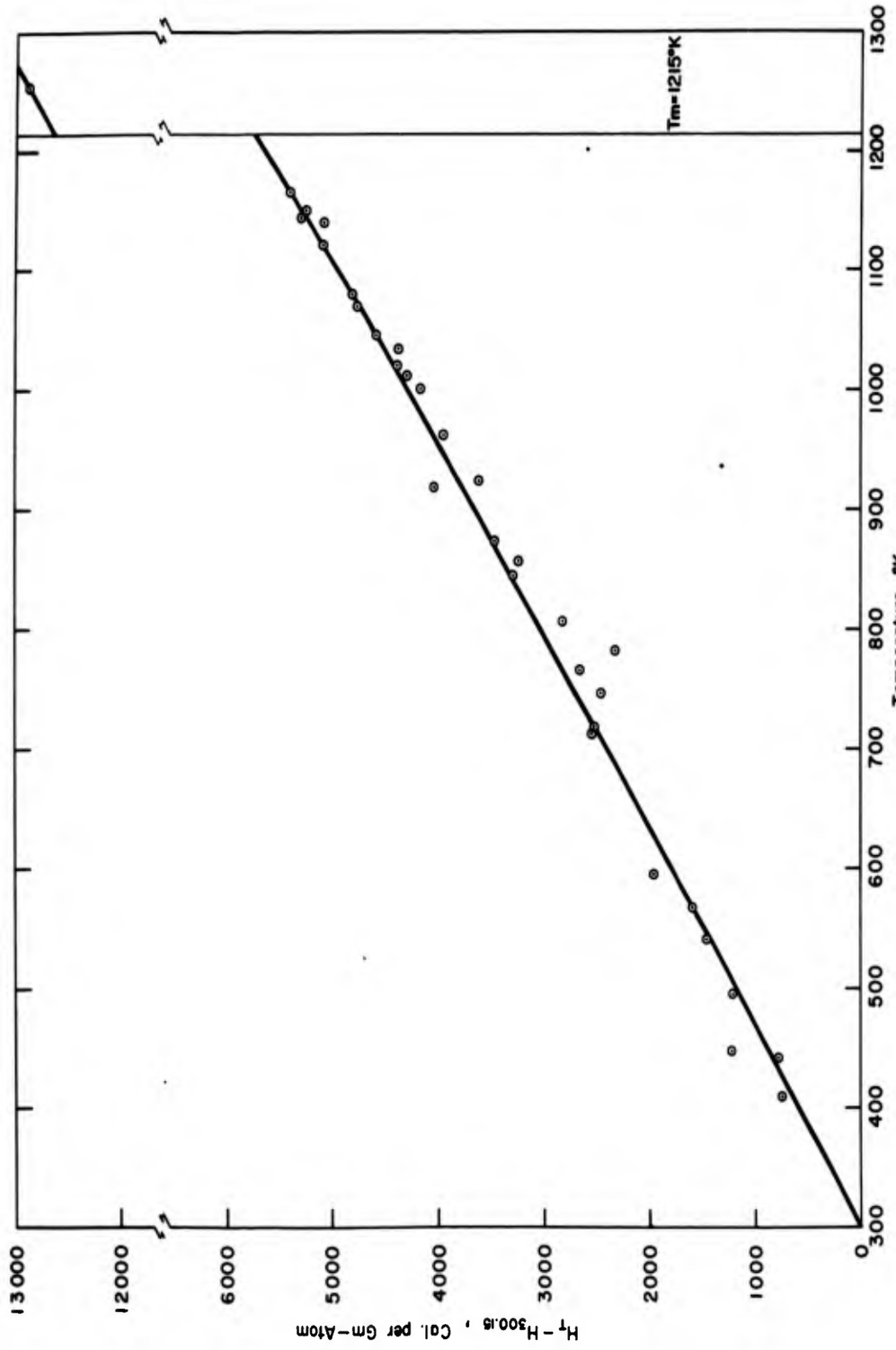

Figure 10. Heat Content of InAs.

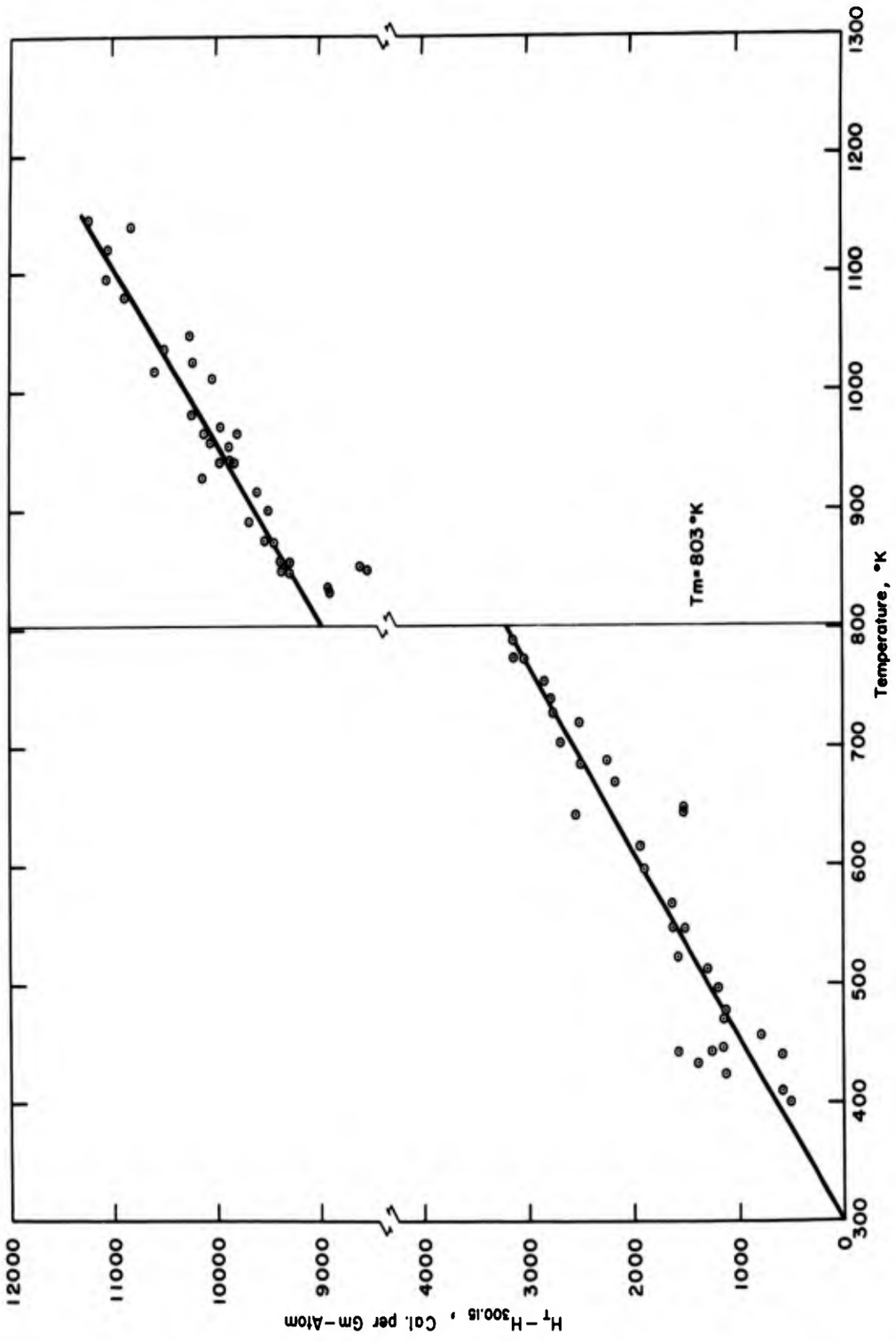

Figure 11. Heat Content of InSb.

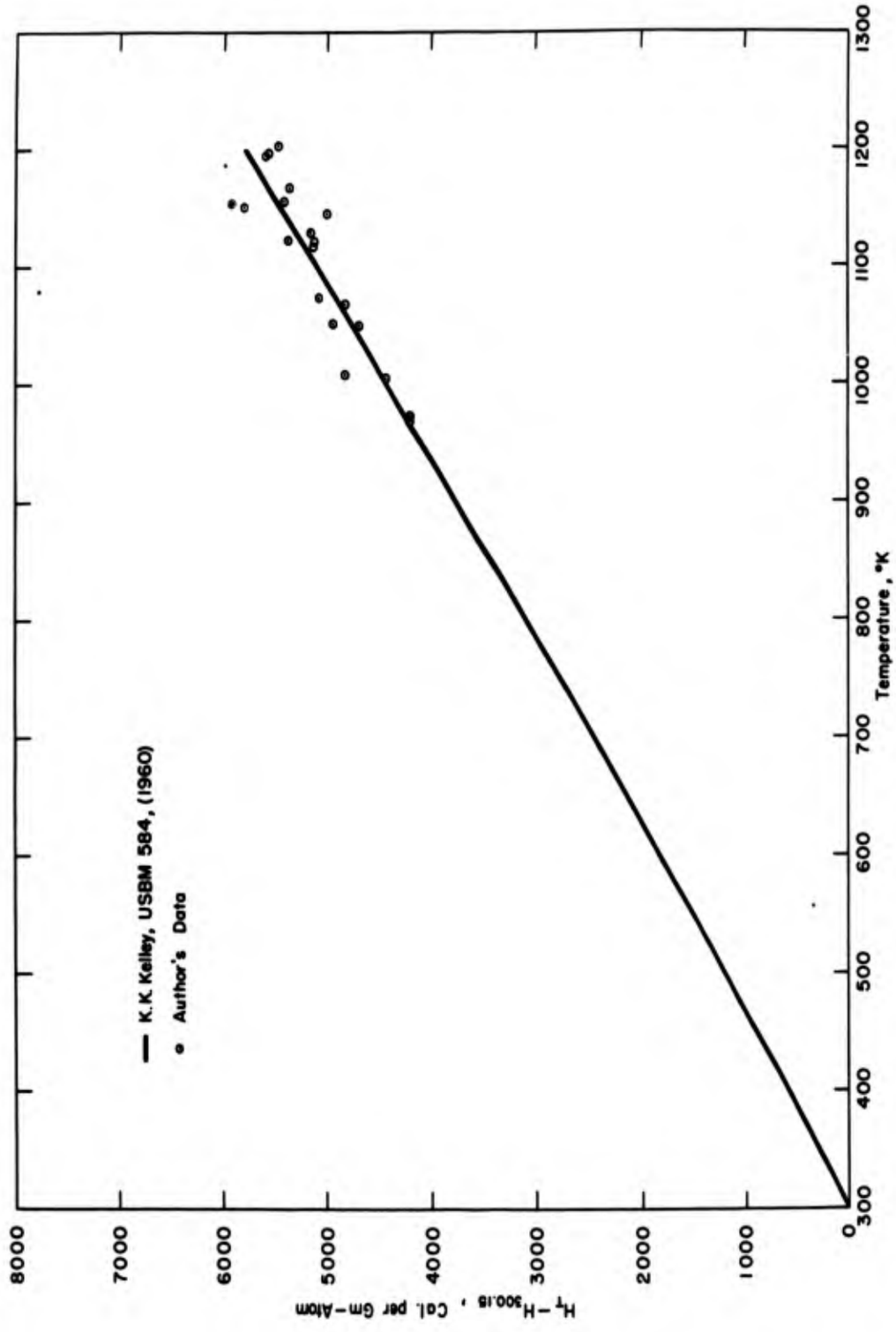

Figure 12. Heat Content of Mo.

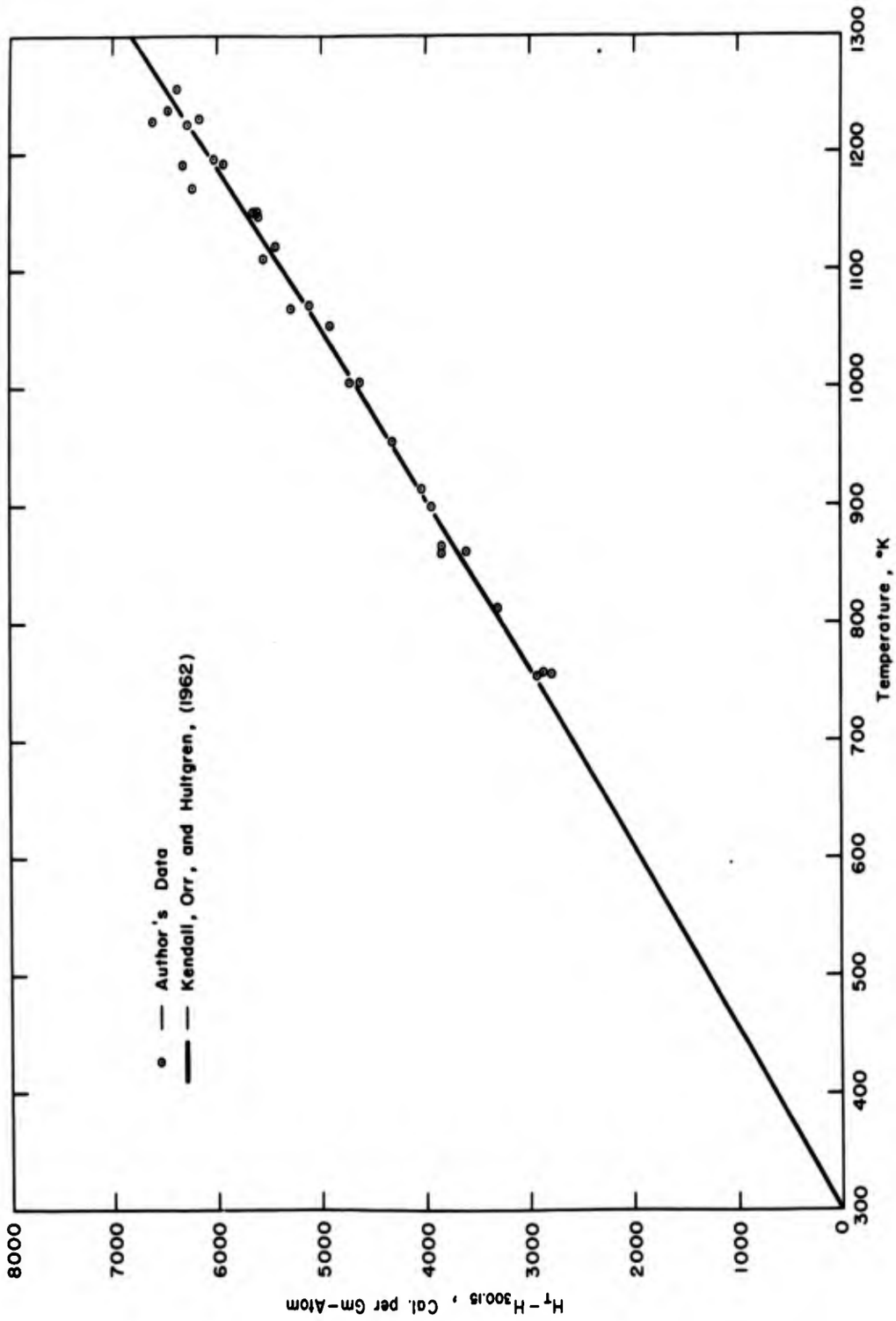

Figure 13. Heat Content of Pt.

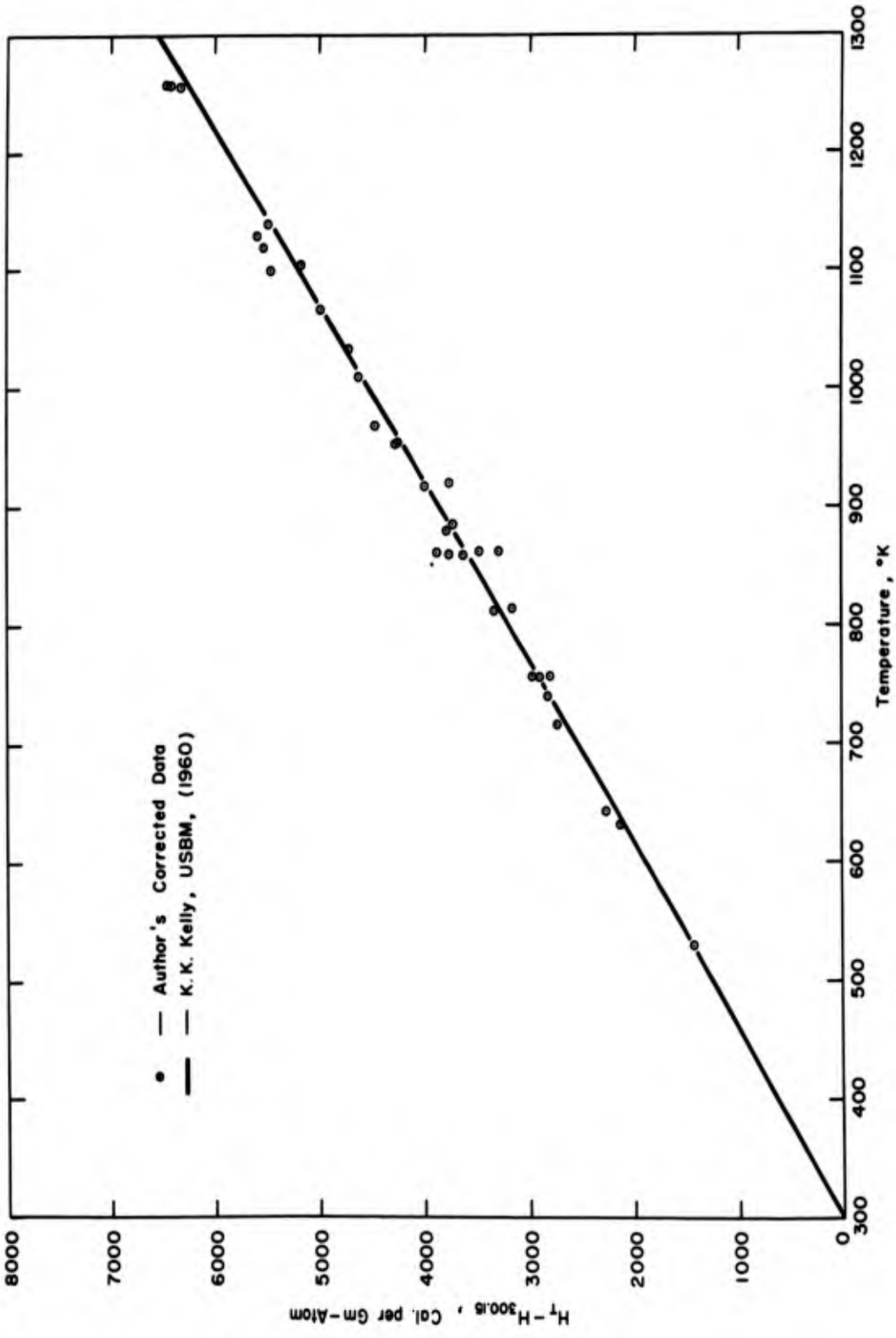

Figure 14. Heat Content of Ta.

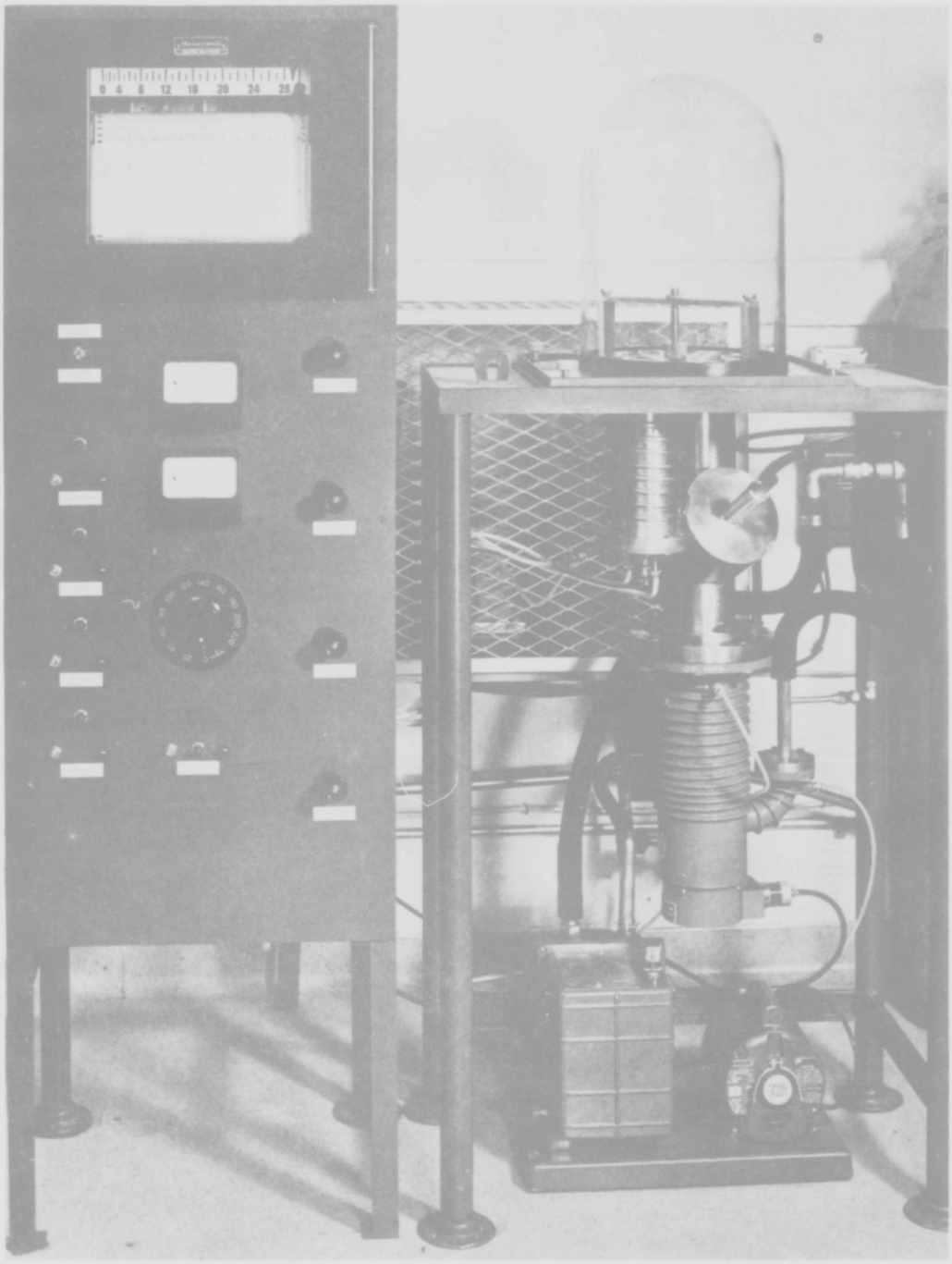

Figure 15. Knudsen Effusion Apparatus.

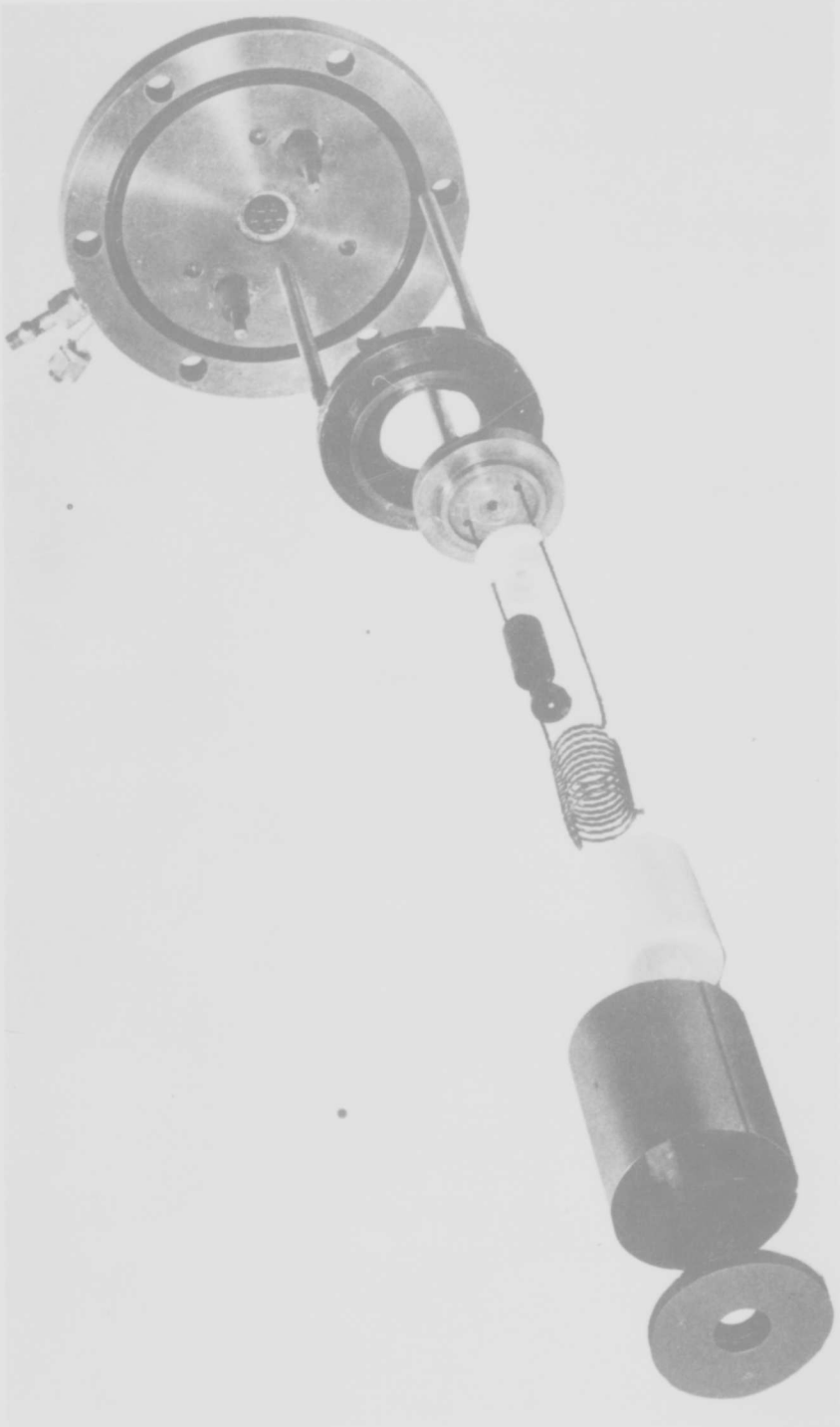

Figure 16. Knudsen Furnace, Effusion Cell, and Components.

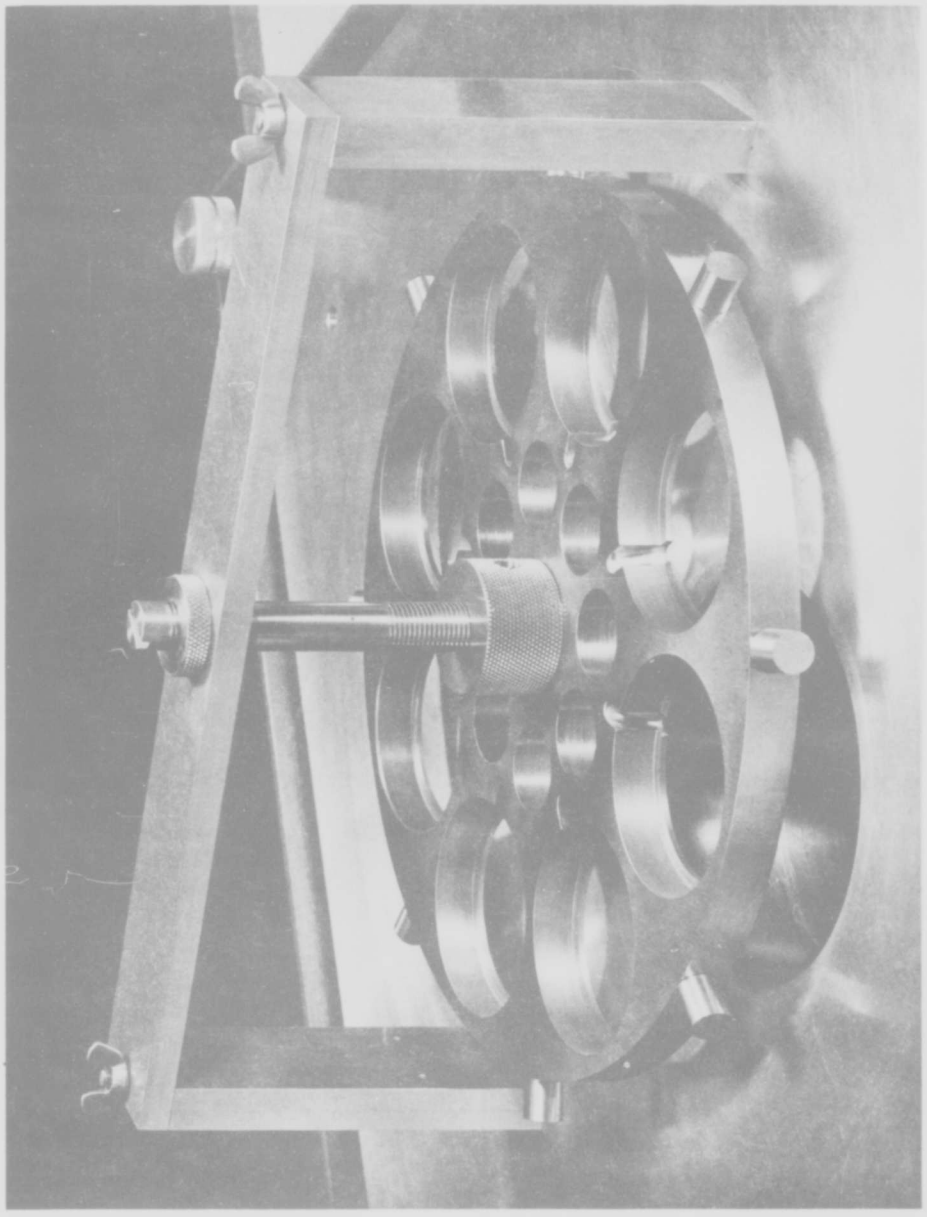

Figure 17. Target Wheel Assembly.

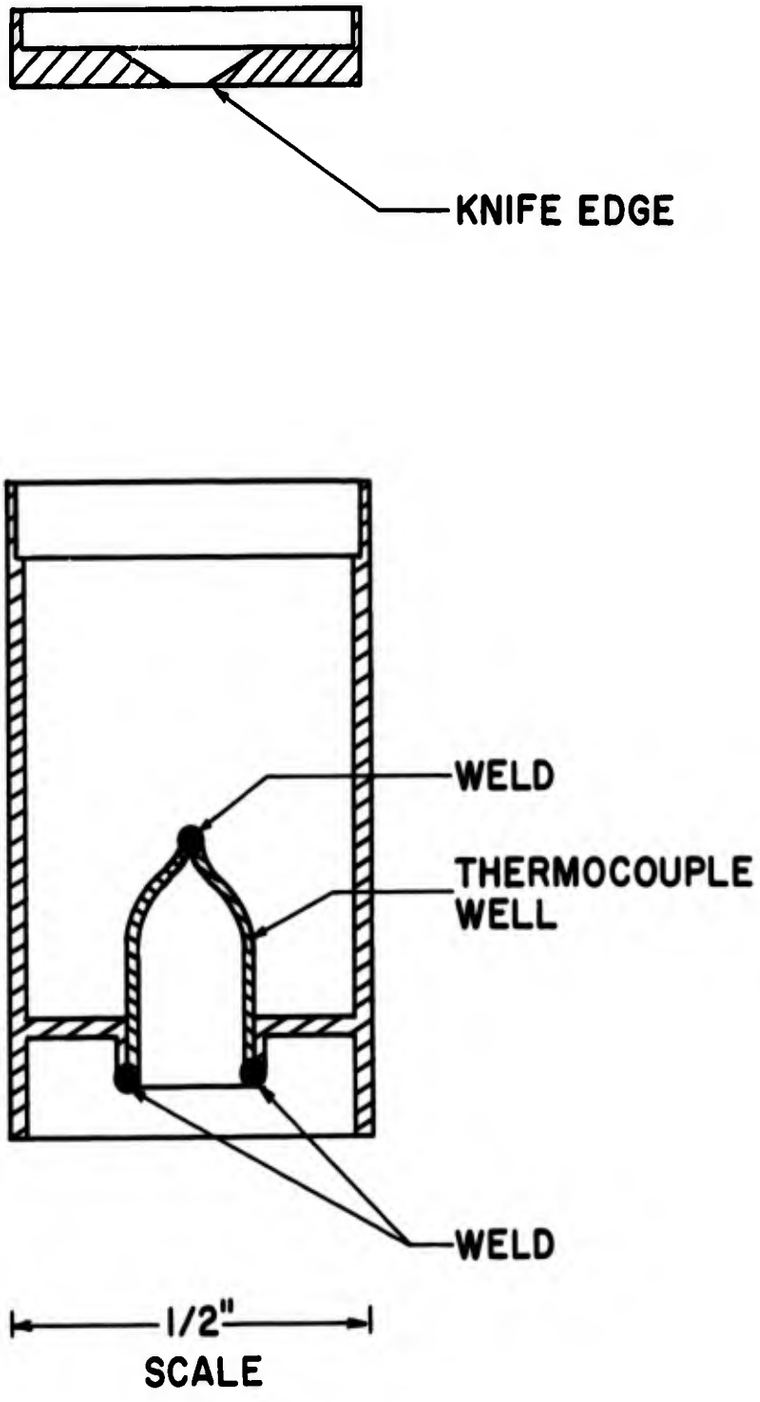

Figure 18. Cross Section of Tantalum Effusion Cell and Lid.

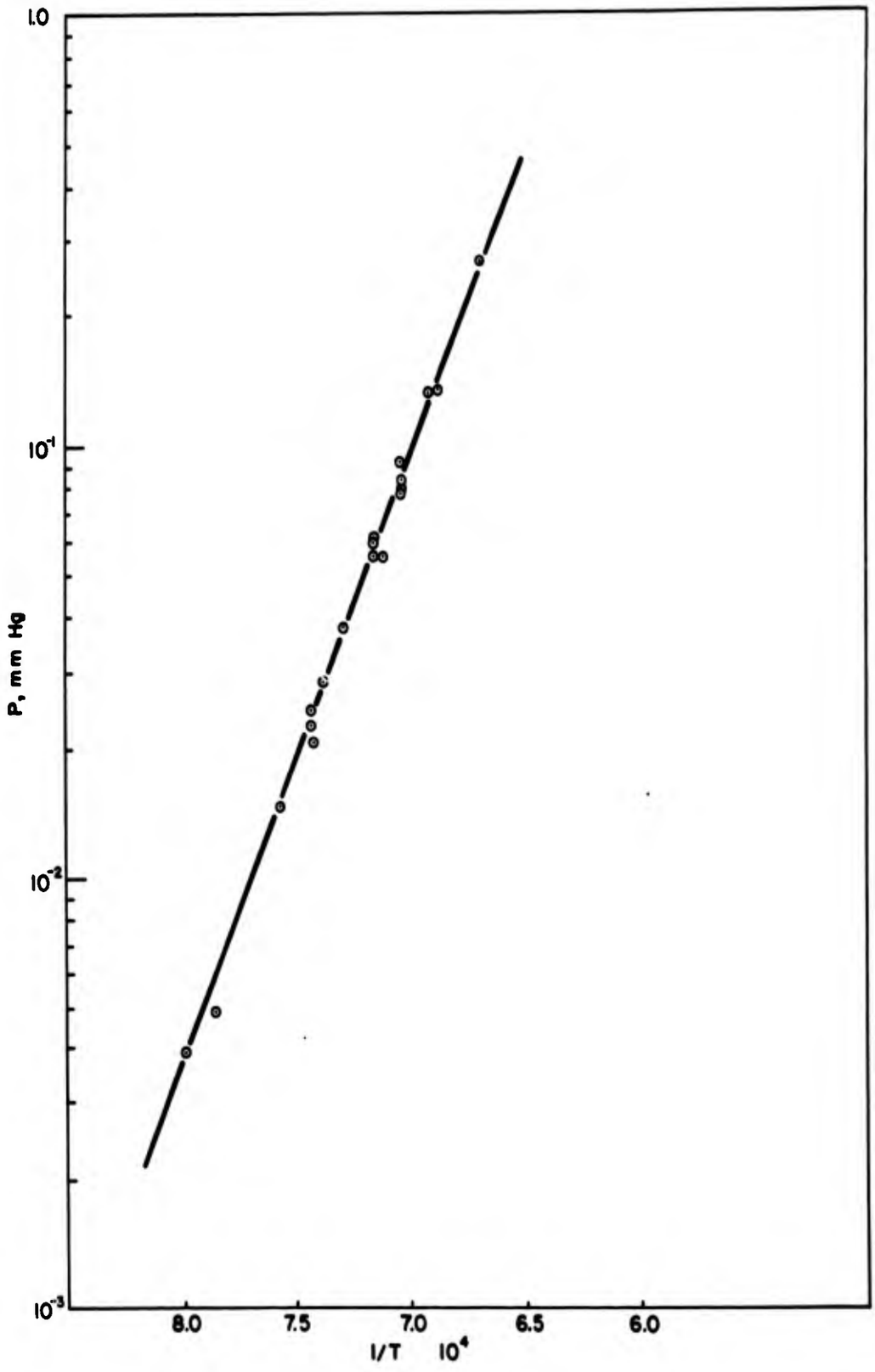

Figure 19. Vapor Pressure of Silver.

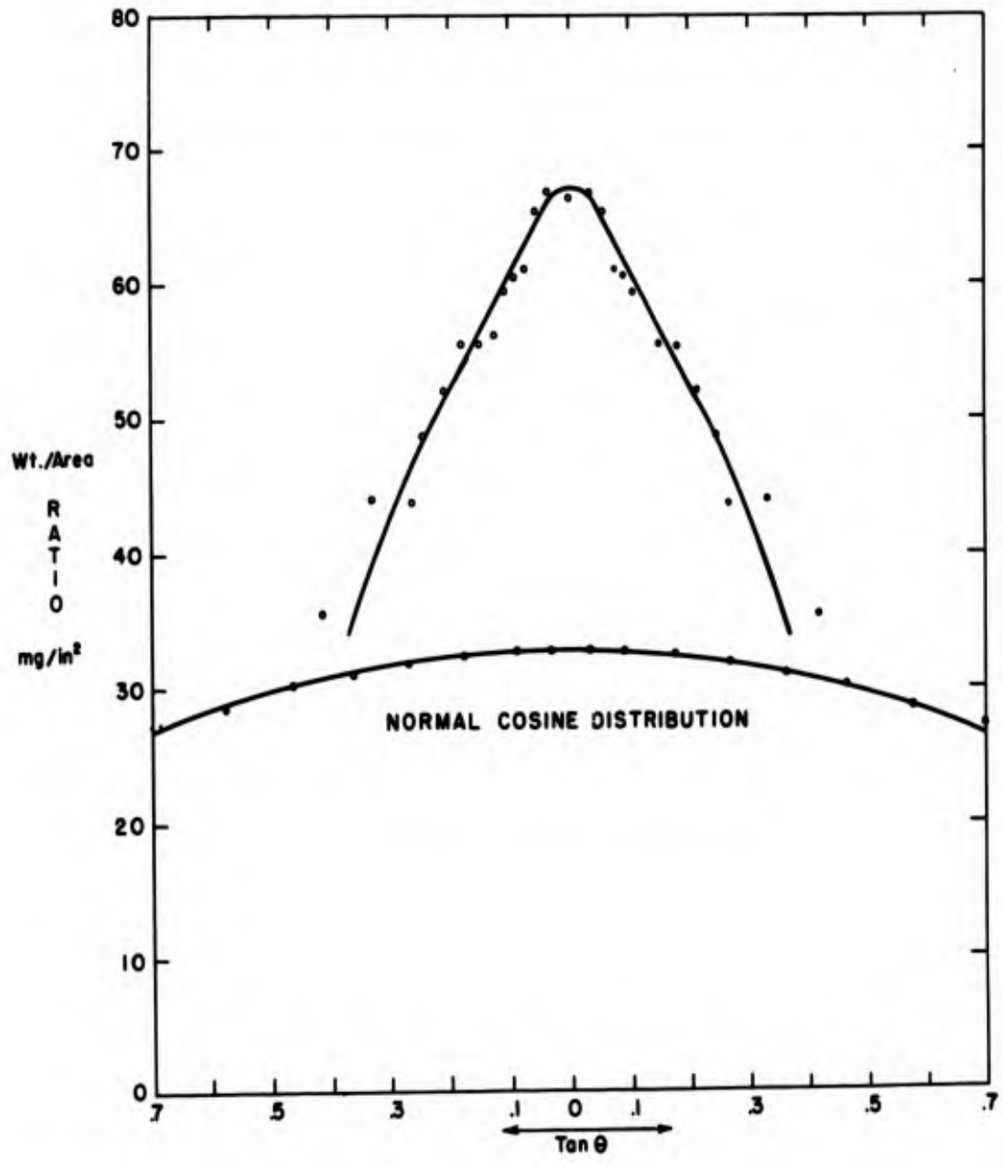

Figure 20. Vapor Distribution Pattern.

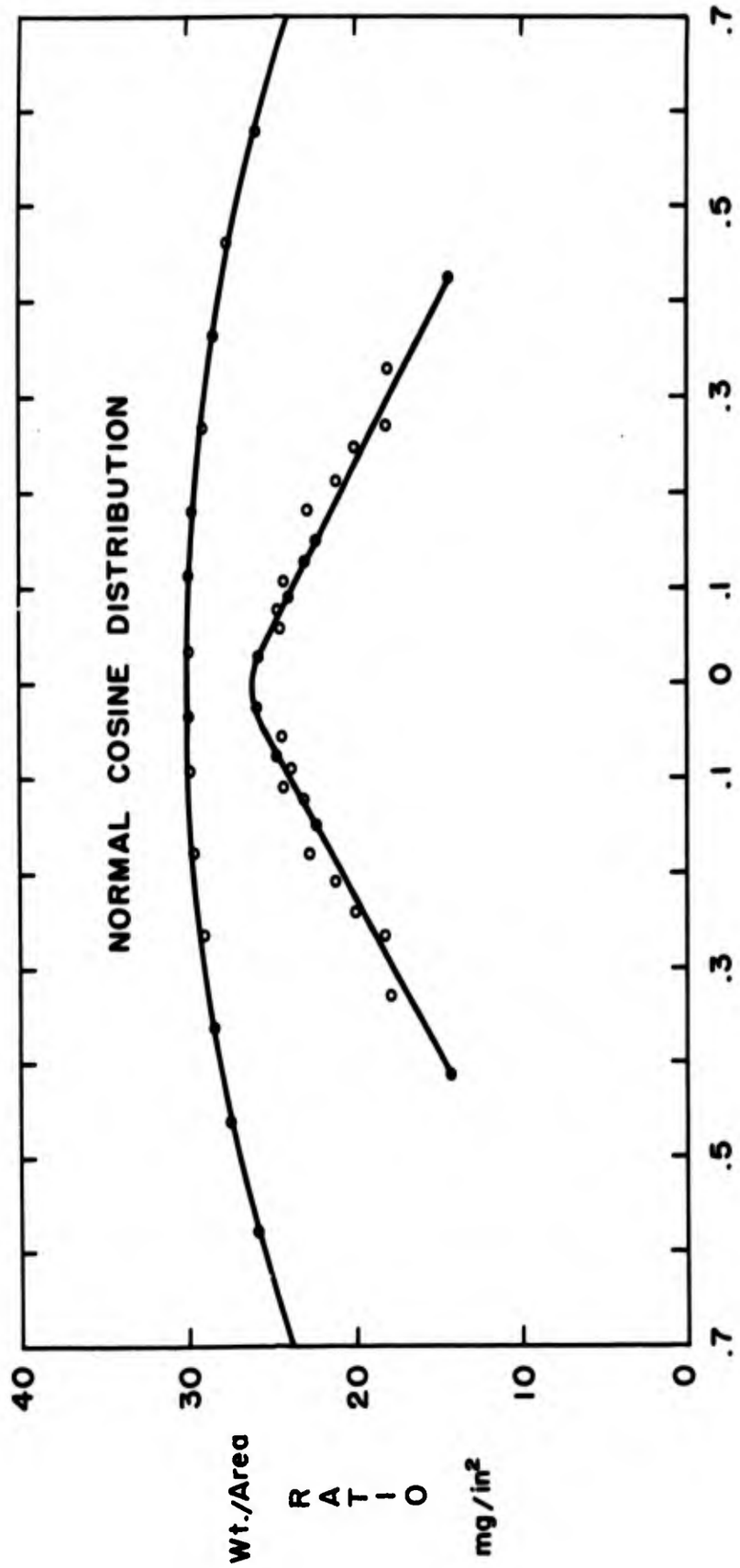

Figure 21. Vapor Distribution Pattern With New Geometry.

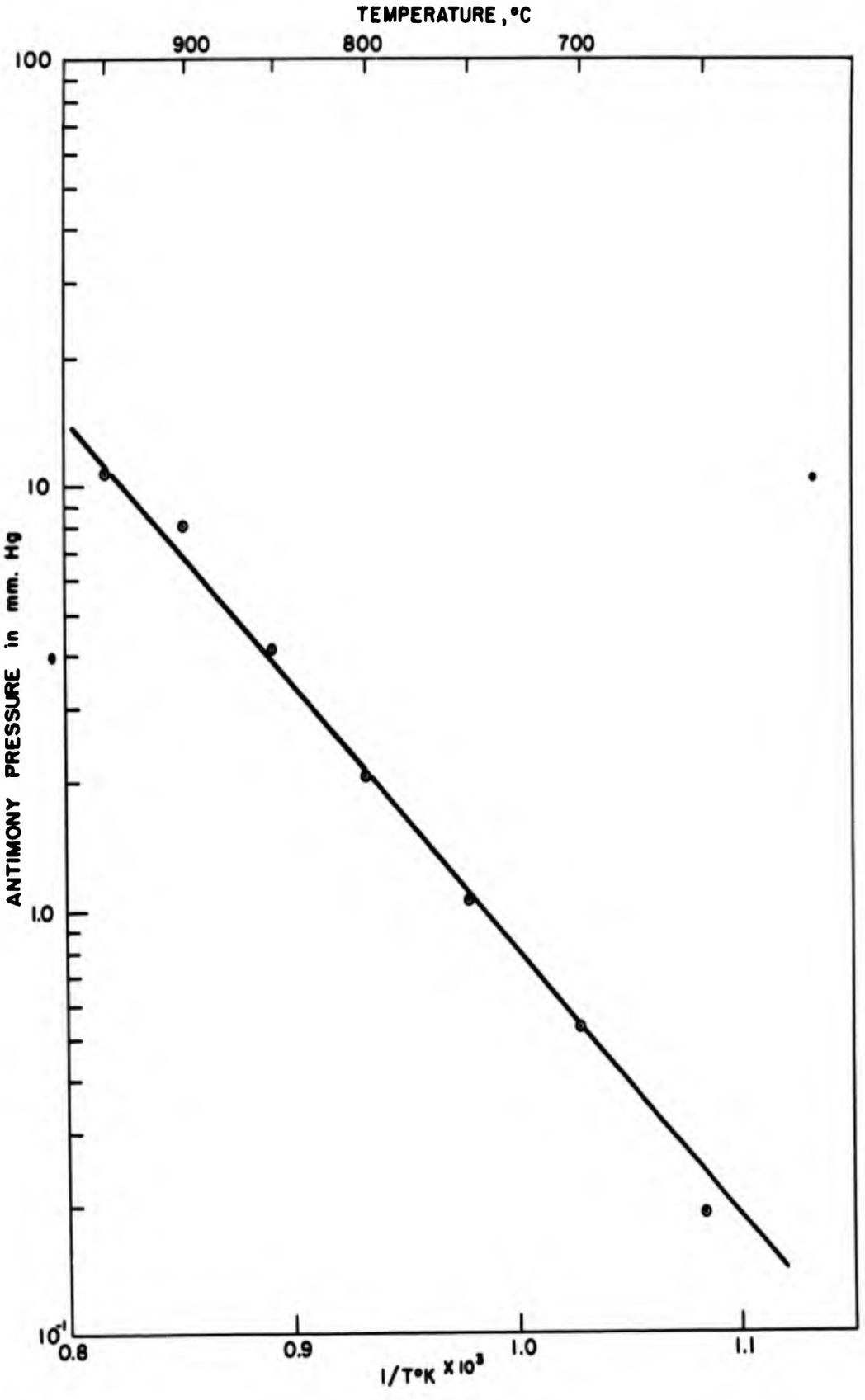

Figure 22. Vapor Pressure of Antimony.

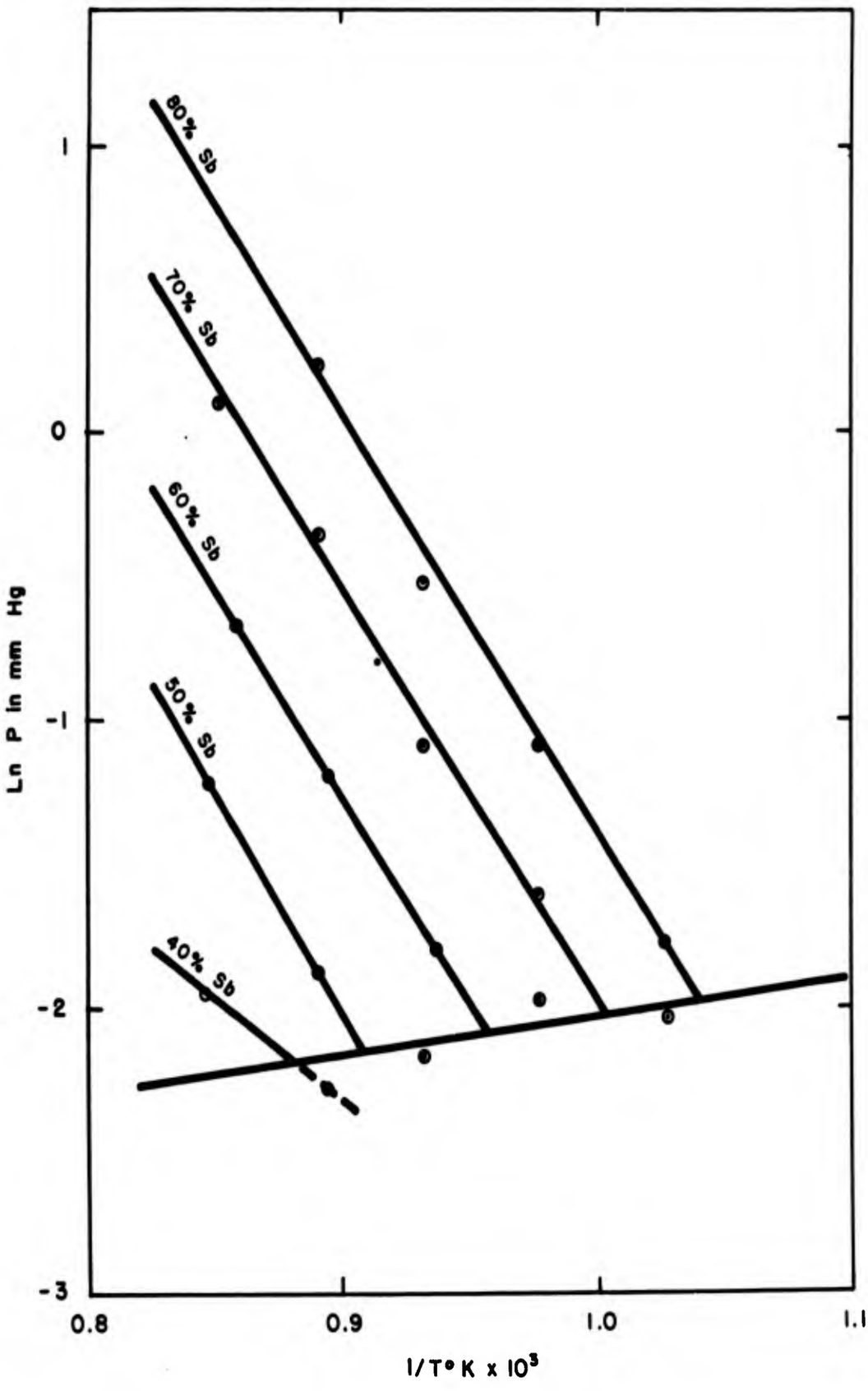

Figure 23. Vapor Pressure Curves for the Germanium-Antimony System.

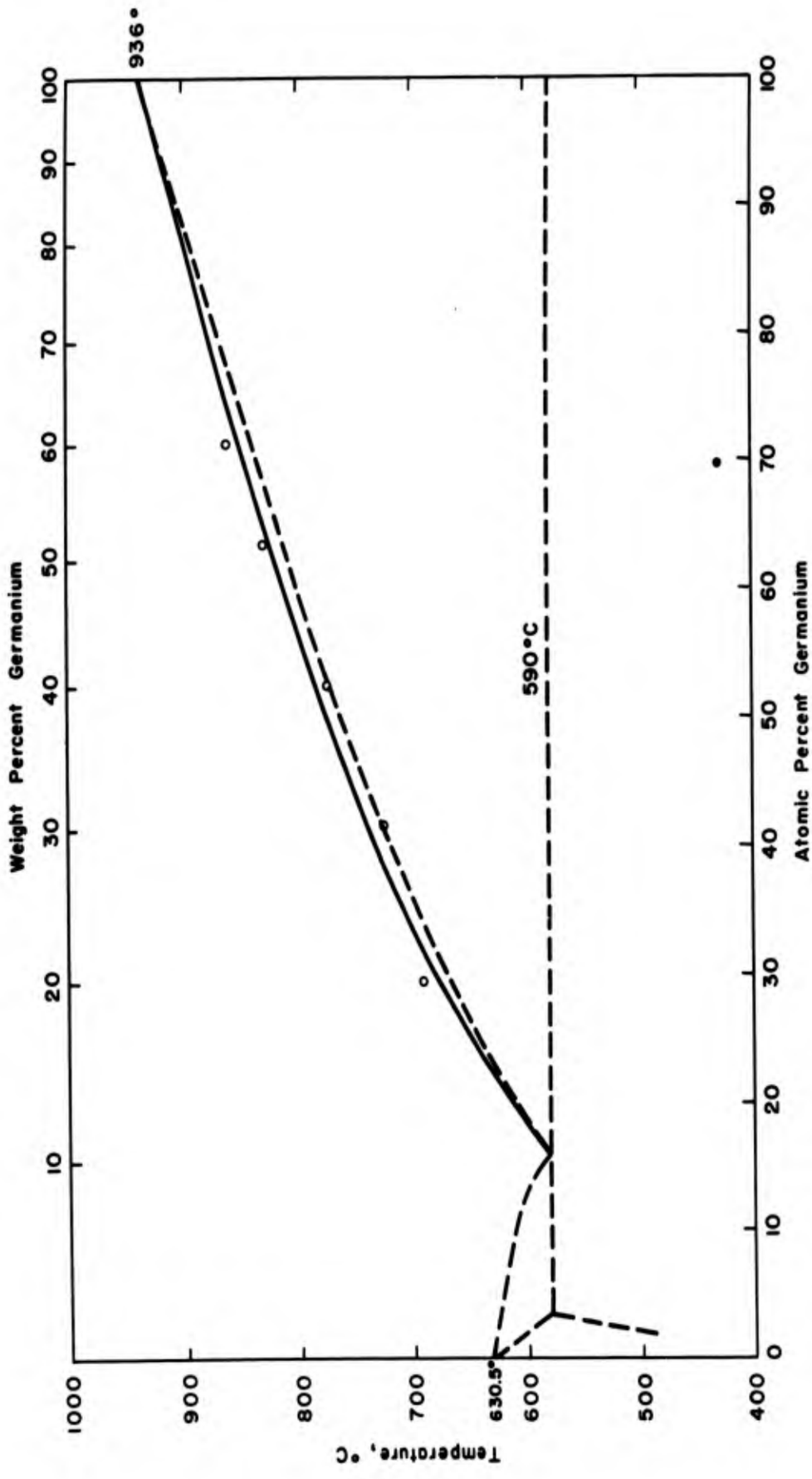

Figure 24. The Liquidus Boundary of the Germanium-Antimony System as Determined from the Vapor Pressure Data.

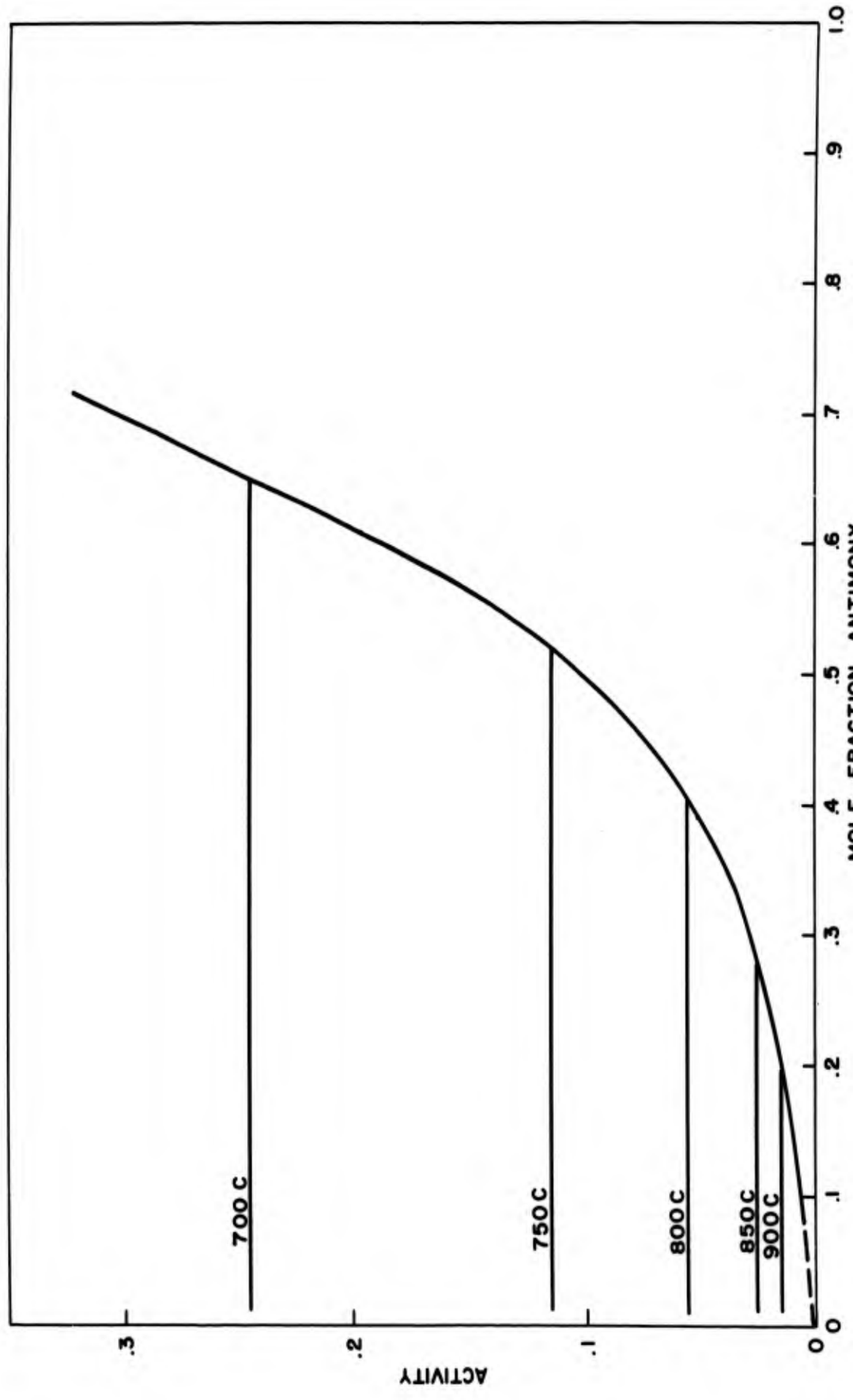

Figure 25. Family of Activity Curves for the Germanium-Antimony System.

A. F. Cambridge Research Laboratories
Bedford, Massachusetts
DETERMINATION OF THERMODYNAMIC PROPERTIES OF SEMICONDUCTOR MATERIALS, by C. E. Lundin, M. J. Pool, R. W. Sullivan, May 1963, pp. 55
AFCRL-63-156 Unclassified Report

A diphenyl ether calorimeter and a liquid-tin solution calorimeter were employed to determine selected thermodynamic properties of Group III and V elements and their compounds. The enthalpy and heat capacity of eight Group III-V compounds were determined in the solid state. The compounds are: InP, InAs, InSb, GaP, GaAs, GaSb, AlP, and AlSb. Data were obtained on the enthalpy and heat capacity of the liquids of several of these compounds. The heat of fusion was then

UNCLASSIFIED

1. Thermodynamics
2. Semiconductor Materials

1. C. E. Lundin
2. M. J. Pool
3. R. W. Sullivan

UNCLASSIFIED

A. F. Cambridge Research Laboratories
Bedford, Massachusetts
DETERMINATION OF THERMODYNAMIC PROPERTIES OF SEMICONDUCTOR MATERIALS, by C. E. Lundin, M. J. Pool, R. W. Sullivan, May 1963, pp. 55
AFCRL-63-156 Unclassified Report

A diphenyl ether calorimeter and a liquid-tin solution calorimeter were employed to determine selected thermodynamic properties of Group III and V elements and their compounds. The enthalpy and heat capacity of eight Group III-V compounds were determined in the solid state. The compounds are: InP, InAs, InSb, GaP, GaAs, GaSb, AlP, and AlSb. Data were obtained on the enthalpy and heat capacity of the liquids of several of these compounds. The heat of fusion was then

UNCLASSIFIED

1. Thermodynamics
2. Semiconductor Materials

1. C. E. Lundin
2. M. J. Pool
3. R. W. Sullivan

UNCLASSIFIED

calculated for these several compounds. The heats of solution of the elements: Al, Ga, In, P, As, and Sb and the compounds: GaSb, InP, InAs, and InSb in tin were determined. From these data the heats of formation of the same compounds were determined.

Knudsen effusion studies were conducted on pure antimony and a series of alloys of the antimony-germanium systems. The vapor pressure of pure antimony was first determined in the range of temperature, 700 to 900C. Vapor pressures and activities of antimony over the mixtures of these alloys were then established. Heats of vaporization for both pure antimony and of antimony over the alloys are presented. The liquid/liquid plus solid boundary of the phase diagram was established from the plot of activity versus mole fraction.

UNCLASSIFIED

calculated for these several compounds. The heats of solution of the elements: Al, Ga, In, P, As, and Sb and the compounds: GaSb, InP, InAs, and InSb in tin were determined. From these data the heats of formation of the same compounds were determined.

Knudsen effusion studies were conducted on pure antimony and a series of alloys of the antimony-germanium systems. The vapor pressure of pure antimony was first determined in the range of temperature, 700 to 900C. Vapor pressures and activities of antimony over the mixtures of these alloys were then established. Heats of vaporization for both pure antimony and of antimony over the alloys are presented. The liquid/liquid plus solid boundary of the phase diagram was established from the plot of activity versus mole fraction.

UNCLASSIFIED

A. F. Cambridge Research Laboratories
Bedford, Massachusetts
DETERMINATION OF THERMODYNAMIC PROPERTIES OF SEMICONDUCTOR MATERIALS, by C. E. Lundin, M. J. Pool, R. W. Sullivan, May 1963, pp. 55
AFCRL-63-156 Unclassified Report

A diphenyl ether calorimeter and a liquid-tin solution calorimeter were employed to determine selected thermodynamic properties of Group III and V elements and their compounds. The enthalpy and heat capacity of eight Group III-V compounds were determined in the solid state. The compounds are: InP, InAs, InSb, GaP, GaAs, GaSb, AlP, and AlSb. Data were obtained on the enthalpy and heat capacity of the liquids of several of these compounds. The heat of fusion was then calculated for these several compounds. The heats of solution of the elements: Al, Ga, In, P, As, and Sb and the compounds: GaSb, InP, InAs, and InSb in tin were determined. From these data the heats of formation of the same compounds were determined.

Knudsen effusion studies were conducted on pure antimony and a series of alloys of the antimony-germanium systems. The vapor pressure of pure antimony was first determined in the range of temperature, 700 to 900C. Vapor pressures and activities of antimony over the mixtures of these alloys were then established. Heats of vaporization for both pure antimony and of antimony over the alloys are presented. The liquid/liquid plus solid boundary of the phase diagram was established from the plot of activity versus mole fraction.

UNCLASSIFIED

1. Thermodynamics
2. Semiconductor Materials

1. C. E. Lundin
2. M. J. Pool
3. R. W. Sullivan

UNCLASSIFIED

UNCLASSIFIED

A. F. Cambridge Research Laboratories
Bedford, Massachusetts
DETERMINATION OF THERMODYNAMIC PROPERTIES OF SEMICONDUCTOR MATERIALS, by C. E. Lundin, M. J. Pool, R. W. Sullivan, May 1963, pp. 55
AFCRL-63-156 Unclassified Report

A diphenyl ether calorimeter and a liquid-tin solution calorimeter were employed to determine selected thermodynamic properties of Group III and V elements and their compounds. The enthalpy and heat capacity of eight Group III-V compounds were determined in the solid state. The compounds are: InP, InAs, InSb, GaP, GaAs, GaSb, AlP, and AlSb. Data were obtained on the enthalpy and heat capacity of the liquids of several of these compounds. The heat of fusion was then calculated for these several compounds. The heats of solution of the elements: Al, Ga, In, P, As, and Sb and the compounds: GaSb, InP, InAs, and InSb in tin were determined. From these data the heats of formation of the same compounds were determined.

Knudsen effusion studies were conducted on pure antimony and a series of alloys of the antimony-germanium systems. The vapor pressure of pure antimony was first determined in the range of temperature, 700 to 900C. Vapor pressures and activities of antimony over the mixtures of these alloys were then established. Heats of vaporization for both pure antimony and of antimony over the alloys are presented. The liquid/liquid plus solid boundary of the phase diagram was established from the plot of activity versus mole fraction.

UNCLASSIFIED

1. Thermodynamics
2. Semiconductor Materials

1. C. E. Lundin
2. M. J. Pool
3. R. W. Sullivan

UNCLASSIFIED

UNCLASSIFIED

UNCLASSIFIED